

# MODERN PATHOLOGY

## ABSTRACTS

PANCREAS, GALLBLADDER, AMPULLA,  
AND EXTRA-HEPATIC BILIARY TREE  
(863-890)

USCAP 110TH ANNUAL MEETING  
**NEVER STOP**  
**LEARNING**  
**2021**



MARCH 13-18, 2021

VIRTUAL AND INTERACTIVE

Published by  
**SPRINGER NATURE**  
[www.ModernPathology.org](http://www.ModernPathology.org)

 **USCAP** AN OFFICIAL JOURNAL OF THE  
UNITED STATES AND CANADIAN  
ACADEMY OF PATHOLOGY  
Creating a Better Pathologist



EDUCATION COMMITTEE

Jason L. Hornick  
Chair

Rhonda K. Yantiss, Chair  
Abstract Review Board and Assignment Committee

Kristin C. Jensen  
Chair, CME Subcommittee

Laura C. Collins  
Interactive Microscopy Subcommittee

Raja R. Seethala  
Short Course Coordinator

Ilan Weinreb  
Subcommittee for Unique Live Course Offerings

David B. Kaminsky  
(Ex-Officio)  
Zubair W. Baloch  
Daniel J. Brat  
Sarah M. Dry  
William C. Faquin  
Yuri Fedoriw  
Karen Fritchie  
Jennifer B. Gordetsky  
Melinda Lerwill  
Anna Marie Mulligan

Liron Pantanowitz  
David Papke,  
Pathologist-in-Training  
Carlos Parra-Herran  
Rajiv M. Patel  
Deepa T. Patil  
Charles Matthew Quick  
Lynette M. Sholl  
Olga K. Weinberg  
Maria Westerhoff  
Nicholas A. Zoumberos,  
Pathologist-in-Training

ABSTRACT REVIEW BOARD

Benjamin Adam  
Rouba Ali-Fehmi  
Daniela Allende  
Ghassan Allo  
Isabel Alvarado-Cabrero  
Catalina Amador  
Tatjana Antic  
Roberto Barrios  
Rohit Bhargava  
Luiz Blanco  
Jennifer Boland  
Alain Borczuk  
Elena Brachtel  
Marilyn Bui  
Eric Burks  
Shelley Caltharp  
Wenqing (Wendy) Cao  
Barbara Centeno  
Joanna Chan  
Jennifer Chapman  
Yunn-Yi Chen  
Hui Chen  
Wei Chen  
Sarah Chiang  
Nicole Cipriani  
Beth Clark  
Alejandro Contreras  
Claudiu Cotta  
Jennifer Cotter  
Sonika Dahiya  
Farbod Darvishian  
Jessica Davis  
Heather Dawson  
Elizabeth Demicco  
Katie Dennis  
Anand Dighe  
Suzanne Dintzis  
Michelle Downes

Charles Eberhart  
Andrew Evans  
Julie Fanburg-Smith  
Michael Feely  
Dennis Firchau  
Gregory Fishbein  
Andrew Folpe  
Larissa Furtado  
Billie Fyfe-Kirschner  
Giovanna Giannico  
Christopher Giffith  
Anthony Gill  
Paula Ginter  
Tamar Giorgadze  
Purva Gopal  
Abha Goyal  
Rondell Graham  
Alejandro Gru  
Nilesh Gupta  
Mamta Gupta  
Gillian Hale  
Suntrea Hammer  
Malini Harigopal  
Douglas Hartman  
Kammi Henriksen  
John Higgins  
Mai Hoang  
Aaron Huber  
Doina Ivan  
Wei Jiang  
Vickie Jo  
Dan Jones  
Kirk Jones  
Neerja Kambham  
Dipti Karamchandani  
Nora Katabi  
Darcy Kerr  
Francesca Khani

Joseph Khoury  
Rebecca King  
Veronica Klepeis  
Christian Kunder  
Steven Lagana  
Keith Lai  
Michael Lee  
Cheng-Han Lee  
Madelyn Lew  
Faqian Li  
Ying Li  
Haiyan Liu  
Xiuli Liu  
Lesley Lomo  
Tamara Lotan  
Sebastian Lucas  
Anthony Magliocco  
Kruti Maniar  
Brock Martin  
Emily Mason  
David McClintock  
Anne Mills  
Richard Mitchell  
Neda Moatamed  
Sara Monaco  
Atis Muehlenbachs  
Bita Naini  
Dianna Ng  
Tony Ng  
Michiya Nishino  
Scott Owens  
Jacqueline Parai  
Avani Pendse  
Peter Pytel  
Stephen Raab  
Stanley Radio  
Emad Rakha  
Robyn Reed

Michelle Reid  
Natasha Rekhman  
Jordan Reynolds  
Andres Roma  
Lisa Rooper  
Avi Rosenberg  
Esther (Diana) Rossi  
Souzan Sanati  
Gabriel Sica  
Alexa Siddon  
Deepika Sirohi  
Kalliopi Siziopikou  
Maxwell Smith  
Adrian Suarez  
Sara Szabo  
Julie Teruya-Feldstein  
Khin Thway  
Rashmi Tondon  
Jose Torrealba  
Gary Tozbikian  
Andrew Turk  
Evi Vakiani  
Christopher VandenBussche  
Paul VanderLaan  
Hannah Wen  
Sara Wobker  
Kristy Wolniak  
Shaofeng Yan  
Huihui Ye  
Yunshin Yeh  
Anjana Yeldandi  
Gloria Young  
Lei Zhao  
Minghao Zhong  
Yaolin Zhou  
Hongfa Zhu

To cite abstracts in this publication, please use the following format: **Author A, Author B, Author C, et al. Abstract title (abs#). In "File Title." *Modern Pathology* 2021; 34 (suppl 2): page#**

**863 CDX2 and SATB2 in Pancreatic Ductal Adenocarcinoma: Expression and Prognostic Significance**

Caroline Bsirini<sup>1</sup>, Irene Chen<sup>2</sup>, Mark Ettel<sup>3</sup>, Phoenix Bell<sup>4</sup>, Jennifer Findeis-Hosey<sup>2</sup>, Richard Dunne<sup>3</sup>, Michael Drage<sup>2</sup>, Diana Agostini-Vulaj<sup>2</sup>

<sup>1</sup>Emory University Hospital, Atlanta, GA, <sup>2</sup>University of Rochester Medical Center, Rochester, NY, <sup>3</sup>University of Rochester, Rochester, NY, <sup>4</sup>Brigham and Women's Hospital, Harvard Medical School, Boston, MA

**Disclosures:** Caroline Bsirini: None; Irene Chen: None; Mark Ettel: None; Phoenix Bell: None; Jennifer Findeis-Hosey: None; Richard Dunne: None; Michael Drage: None; Diana Agostini-Vulaj: None

**Background:** The caudal-related homeobox transcription factor2 (CDX2) is an intestine specific transcription factor involved in intestinal epithelial proliferation and differentiation. Special AT-rich binding protein-2 (SATB2) is a novel transcription factor that is involved in chromatin remodeling and transcription regulation and has been shown to be expressed in most colorectal and appendiceal adenocarcinomas. Most routine use of CDX2 and SATB2 immunostaining has been to support colorectal origin in metastatic carcinomas of unknown primary. There are very limited studies that have evaluated CDX2 and SATB2 expression and any prognostic implications in pancreatic ductal adenocarcinoma (PDAC). Thus, the aim of this study was to examine the expression, clinicopathological correlates, and prognosis of CDX2 and SATB2 in PDACs.

**Design:** A tissue microarray with 374 PDACs was evaluated for the expression of CDX2 and SATB2 by immunohistochemistry. The intensity and percent expression of CDX2 and SATB2 staining was recorded. For CDX2 positive cases, an H-score was calculated, those with a score of ≥200 were defined as high expressers. Clinicopathologic parameters were recorded including tumor size, margin status, histologic grade, pathologic stage, perineural invasion, lymphovascular invasion, progression free survival, and overall survival. As appropriate, statistical analyses were performed using t-test, Fisher test, Kruskal-Wallis, and log-rank with p-values <0.05 considered statistically significant.

**Results:** High CDX2 expression was seen in 13 (4%) of 356 evaluable PDACs, these cases were associated with smaller tumor size (p= 0.025), less frequent nodal metastases (p= 0.029) and less frequent perineural invasion (p= 0.025) (**Table**). High CDX2 expressers demonstrated better progression free survival and overall survival compared to those with low or no expression (p<0.001 and p=0.001) (**Fig. 1 and 2**). SATB2 expression was seen in 7 (2%) of 357 evaluable PDACs, with strong and diffuse positivity seen in only 1 case. No significant clinicopathologic differences were seen between SATB2 positive and SATB2 negative cases and no significant differences in progression free survival or overall survival were seen (p=0.727 and p=0.062).

	CDX2 High	CDX2 Negative/Low	p-value
Total patients	13	343	
Tumor gross size (cm), <i>mean ± sd</i>	2.8 ± 1.0	3.5 ± 1.7	<b>0.025*</b>
Margin status			1
R0	6 (46.2)	167 (48.7)	
R1	7 (53.8)	176 (51.3)	
Histologic grade			0.321
1	2 (16.7)	33 (9.6)	
2	7 (58.3)	184 (53.8)	
3	3 (25)	123 (36.0)	
4	0 (0)	2 (0.6)	
pT stage, <i>n (%)</i>			0.376
1a	0 (0)	0 (0)	
1b	1 (7.7)	0 (0)	
1c	1 (7.7)	23 (6.7)	
2	8 (61.5)	219 (64.2)	
3	3 (23.1)	99 (29.0)	

4	0 (0)	0 (0)	
pN stage, <i>n</i> (%)			<b>0.029*</b>
0	9 (69.2)	96 (28.0)	
1	1 (7.7)	149 (43.4)	
2	3 (23.1)	98 (28.6)	
pM stage, <i>n</i> (%)			1
0 or X	13 (100)	328 (95.6)	
1	0 (0)	15 (4.4)	
LVI, <i>n</i> (%)	5 (38.5)	208 (61.0)	0.147
PNI, <i>n</i> (%)	9 (69.2)	312 (91.5)	<b>0.025*</b>

Figure 1 - 863

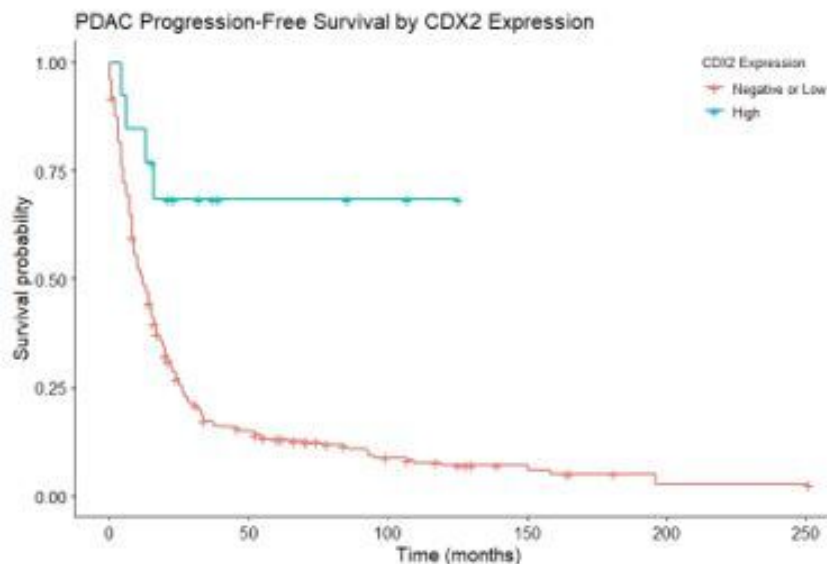
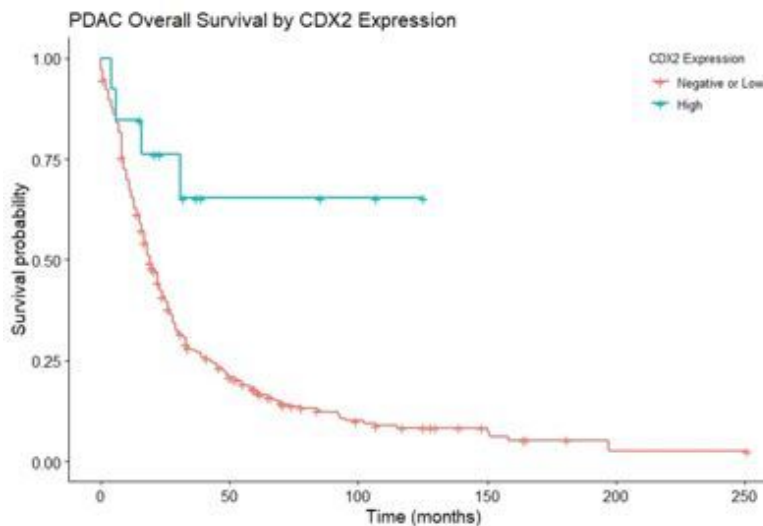


Figure 2 - 863



**Conclusions:** To the best of our knowledge, we present the largest study evaluating SATB2 and CDX2 expression and its prognostic implications in PDAC. Overall, High CDX2 expressers (H score  $\geq 200$ ) correlated with better prognosis and overall survival, with smaller tumor size, less nodal metastases, and less frequent perineural invasion. Less than 2% of our PDACs stained positive for SATB2, with no observed prognostic implications.



**864 KRAS-G12V/G12R Mutations are Associated with Improved Clinical Outcomes and Different Morphological Variants Compared to KRAS-G12D in Pancreatic Ductal Adenocarcinoma**

Timothy Chao<sup>1</sup>, Zixuan Wang<sup>2</sup>, Wilbur Bowne<sup>1</sup>, Clifford Yudkoff<sup>3</sup>, Austin Roadarmel<sup>3</sup>, Ava Torjani<sup>3</sup>, Cyrus Sholevar<sup>3</sup>, Taylor Kavanagh<sup>3</sup>, Vishal Swaminathan<sup>3</sup>, Shawwna Cannaday<sup>2</sup>, Geoffrey Krampitz<sup>1</sup>, Harish Lavu<sup>1</sup>, Charles Yeo<sup>1</sup>, Stephen Peiper<sup>4</sup>, Wei Jiang<sup>1</sup>

<sup>1</sup>Thomas Jefferson University Hospital, Philadelphia, PA, <sup>2</sup>Thomas Jefferson University, Philadelphia, PA, <sup>3</sup>Sidney Kimmel Medical College, Thomas Jefferson University, Philadelphia, PA, <sup>4</sup>Sidney Kimmel Medical College, Philadelphia, PA

**Disclosures:** Timothy Chao: None; Wilbur Bowne: None; Cyrus Sholevar: None; Taylor Kavanagh: None; Vishal Swaminathan: None; Geoffrey Krampitz: None; Wei Jiang: None

**Background:** Mutant KRAS (mKRAS) is the main oncogenic driver in pancreatic ductal adenocarcinomas (PDAs). However, the pathological, clinical, and therapeutic implications of having different mKRAS remain poorly understood. Lack of standardized morphological reporting has further hampered efforts to associate histology with molecular subtypes and clinical outcomes. Here we propose a novel morphological classification system for PDA and identify variants that are enriched with certain mKRAS, which in turn associates with clinical outcomes.

**Design:** Database search identified 111 primary PDAs resected at our institution from 2015-2018 for which a 42 gene mutational panel was performed. Mucinous, undifferentiated, and adenosquamous carcinomas as well as IPMN-associated cancers were excluded. H&E slides used for sequencing were reviewed independently by two pathologists. A classification system was devised where each PDA is assigned as conventional (CV), papillary/large-duct (P/LD, defined as neoplastic glands with papillary structure and/or with length ≥0.5mm), or poorly-differentiated (PD), when said component is >50% of the tumor (Fig 1). Student's t-test was used to compare age, while the Mann-Whitney U-test for histological grades. Categorical enrichments were determined by chi-square and, if significant, Fisher's exact tests. Kaplan-Meier curves and logrank tests were used to compare overall survival (OS). For validation, the OS and morphology were also analyzed for 146 and 122 PDAs in the TCGA cohort, respectively.

**Results:** The mKRAS distribution in our cohort (41% G12D, 34% G12V, 14% G12R, and 10% others) is reflective of literature. Substantial interobserver agreement is observed with the new morphological classification system (Cohen's kappa=0.71). There is significant enrichment of the P/LD variant in G12V (p=0.0004) and G12R (p=0.0036) compared to G12D PDAs. Given their similarities and to satisfy conditions for the chi-square, the G12V and G12R groups are combined into G12V/R, which still has significant enrichment for the P/LD variant (p<0.0001). The "other" group is excluded from subsequent analyses because of its small sample size and heterogeneity. Patients with G12V/R PDAs have improved OS compared to those with G12D (HR 0.54, p=0.044) (Figure 2A). No other variables, including stage and treatment, show significant associations with G12V/R (Table 1). Analysis of the TCGA cohort confirms enrichment of the P/LD variant in G12V/R PDAs (p<0.0001), which also has better OS compared to those with G12D (HR 0.55, p=0.029) (Figure 2B).

Table 1. Associations of clinical and pathological characteristics with different KRAS mutations.

	Our Cohort (n=111)				TCGA (n=146)			
	KRAS-G12D (n=46)	KRAS-G12V/R (n=54)	Other (n=11)	p-value*	KRAS-G12D (n=52)	KRAS-G12V/R (n=51)	Other (n=43)	p-value*
<b>Mean Age</b>	67.0	67.6	68.2	0.75	64.7	63.8	65.6	0.66
<b>Sex</b>				1				0.43
Male	22	26	9		31	26	21	
Female	24	28	2		21	25	22	
<b>Stage</b>				0.82				0.47
1A	2	1	—		1	2	1	
1B	4	9	2		3	1	5	
2A	7	7	3		7	9	6	
2B	22	27	6		40	35	30	
3	10	9	—		1	1	1	
4	1	1	—		—	3	—	

<b>Location</b>				0.82				—
head/ampulla	34	38	8		N/A	N/A	N/A	
body/tail	12	16	3		N/A	N/A	N/A	
<b>Resection status</b>				0.24				0.56
r0	41	52	11		24	30	29	
r1	5	2	0		22	16	9	
r2	—	—	—		2	1	2	
Unknown	—	—	—		4	4	3	
<b>Mean Grade (1-3)</b>	2.36	2.19	2.36	0.35	2.17	2.23	2.02	0.75
<b>LVI</b>				0.39				—
Yes	24	24	5		N/A	N/A	N/A	
No	19	22	6		N/A	N/A	N/A	
Indeterminate	3	8	—		N/A	N/A	N/A	
<b>Morphology</b>				<b>0.00024</b>	(n=48)**	(n=47)**	(n=27)**	<b>&lt;0.00001</b>
CV	20	8	5	ref	32	6	5	ref
P/LD	12	39	3	<b>&lt;0.0001</b>	10	40	21	<b>&lt;0.0001</b>
PD	14	7	3	0.76	6	1	1	1
<b>Treatment</b>				0.094				—
None	12	7	3		N/A	N/A	N/A	
Neoadjuvant only	7	3	—		N/A	N/A	N/A	
Adjuvant only	23	37	7		N/A	N/A	N/A	
Both	4	7	1		N/A	N/A	N/A	
<b>Median OS (days)</b>	682	1266	1214	<b>0.044</b>	460	702	485	<b>0.028</b>

\* Statistical comparisons shown are made only between the KRAS-G12D and KRAS-G12V/R groups, excluding those in the "Other" category. p-values are derived as follows: Student's t-test for age, Mann-Whitney U-test for histological grade, chi-square and, if significant, post-hoc Fisher's exact tests for categorical values with the indicated reference (ref) groups. p-values < 0.05 is considered significant.

\*\* Only 122 of the 146 PDAs from TCGA have whole slide images with adequate quality for morphological analyses.

Figure 1 - 864

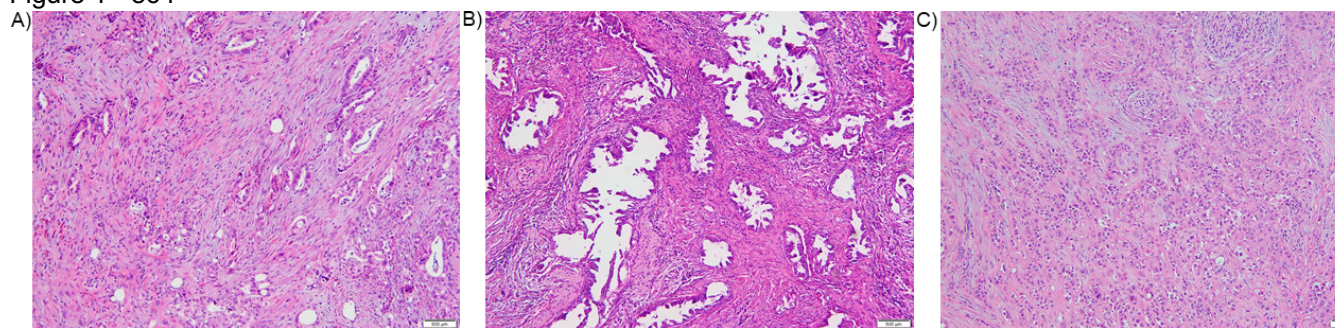
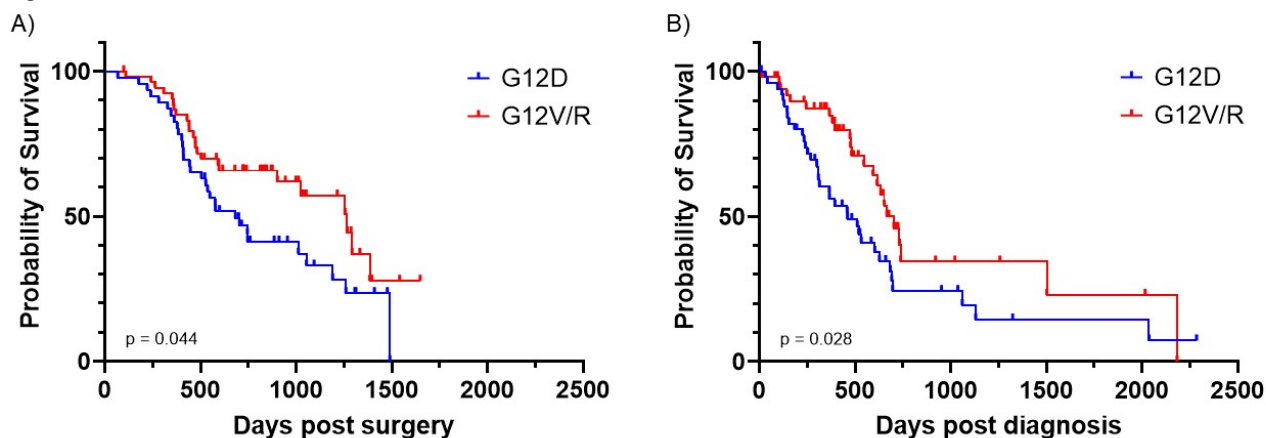


Figure 1. H&E images (10x) showing typical morphologies for the conventional (A), papillary/large-duct (B), and poorly-differentiated (C) variants in pancreatic ductal adenocarcinoma.



Figure 2 - 864



**Figure 2.** Kaplan-Meier curves of overall survival for our institution's cohort (A) and TCGA's cohort (B) showing improved survival of KRAS-G12V/R compared to KRAS-G12D. The p-values from logrank tests are shown.

**Conclusions:** A novel morphological classification system is described and used to demonstrate that PDAs with G12V/R mKRAS are enriched for the P/LD variant. Furthermore, patients with G12V/R PDAs have significantly improved OS as compared to those with G12D. Our work highlights the morphological and clinical significance of different KRAS mutations in PDA.

### 865 SWI/SNF Chromatin Remodeling Complex in Pancreatic Ductal Adenocarcinoma: Clinicopathologic and Immunohistochemical Study of 353 Cases

Irene Chen<sup>1</sup>, Mark Ettl<sup>2</sup>, Phoenix Bell<sup>3</sup>, Aaron Huber<sup>1</sup>, Jennifer Findeis-Hosey<sup>1</sup>, Wenjia Wang<sup>1</sup>, Richard Dunne<sup>2</sup>, Michael Drage<sup>1</sup>, Diana Agostini-Vulaj<sup>1</sup>

<sup>1</sup>University of Rochester Medical Center, Rochester, NY, <sup>2</sup>University of Rochester, Rochester, NY, <sup>3</sup>Brigham and Women's Hospital, Harvard Medical School, Boston, MA

**Disclosures:** Irene Chen: None; Mark Ettl: None; Phoenix Bell: None; Aaron Huber: None; Jennifer Findeis-Hosey: None; Wenjia Wang: None; Richard Dunne: None; Michael Drage: None; Diana Agostini-Vulaj: None

**Background:** The Switch/sucrose non-fermentable (SWI/SNF) complex is a multimeric protein involved in chromatin assembly and repair of DNA damage. Mutations of the SWI/SNF complex are observed in approximately one-third of the pancreatic ductal adenocarcinomas (PDACs). Herein, we evaluated the expression of four SWI/SNF complex proteins (ARID1A, SMARCA4, SMARCA2, and INI1) to determine whether SWI/SNF loss is associated with any clinicopathologic features or patient survival in PDAC.

**Design:** A tissue microarray containing 374 PDACs was stained immunohistochemically using antibodies against ARID1A, SMARCA4, SMARCA2, and INI1. Loss of expression was defined by the complete absence of nuclear staining in tumor nuclei with retained expression in non-neoplastic cells. Clinical and histologic parameters evaluated included patient age, sex, tumor size, margin status, histologic grade, TNM stage, (neo)adjuvant therapy, lymphovascular invasion, perineural invasion, and overall and progression-free survival. Statistical analyses were performed using T-test, Fisher Exact, Kruskal-Wallis, and log-rank tests (p-value <0.05 considered statistically significant).

**Results:** 13 (3.7%) of 353 evaluable PDACs showed deficient SWI/SNF complex expression, which included 11 (3.1%) with ARID1A loss, 1 (0.3%) with SMARCA4 loss, and 1 (0.3%) with SMARCA2 loss. All cases were INI1 proficient. SWI/SNF deficiency was more associated with later onset (median 72 years (range: 58-83)) compared to the SWI/SNF complex proficient PDACs (median 65 years (range 29-88) (p=0.014)). Similar to other cancers, SWI/SNF deficiency was associated with higher histologic grade (**Fig. 1 and 2**) (p=0.030). No other significant clinicopathologic differences were noted between SWI/SNF deficient and SWI/SNF proficient PDACs (**Table**), and

no significant differences were seen with respect to overall survival and progression-free survival between SWI/SNF deficient and proficient PDACs (p=0.447 and p=0.439).

	SWI/SNF Deficient	SWI/SNF Proficient	p-value
Total patients	13	340	
Age, median (range)	72 (58-83)	65 (29-88)	0.014
Sex, n (%)			0.414
Male	5 (38.5)	172 (50.6)	
Female	8 (61.5)	168 (49.4)	
Tumor gross size (cm), mean ± sd	3.8 ± 1.2	3.5 ± 1.7	0.361
Margin status			0.779
R0	7 (53.8)	160 (47.1)	
R1	6 (46.2)	180 (52.9)	
Histologic grade			0.030
1	1 (7.7)	33 (9.8)	
2	3 (23.1)	186 (55.0)	
3	9 (69.2)	117 (34.6)	
4	0 (0)	2 (0.6)	
pT stage, n (%)			0.928
1a	0 (0)	0 (0)	
1b	0 (0)	1 (0.3)	
1c	1 (7.7)	23 (6.8)	
2	8 (61.5)	216 (63.9)	
3	4 (30.8)	98 (29.0)	
4	0 (0)	0 (0)	
pN stage, n (%)			0.766
0	3 (23.1)	99 (29.1)	
1	8 (61.5)	146 (42.9)	
2	2 (15.4)	95 (27.9)	
pM stage, n (%)			0.440
0 or X	12 (92.3)	323 (95.8)	
1	1 (7.7)	14 (4.2)	
LVI, n (%)	10 (76.9)	203 (60.2)	0.262
PNI, n (%)	13 (100)	306 (90.8)	0.618
Treated, n (%)			0.085
Neoadjuvant only	2 (22.2)	18 (6.0)	
Adjuvant only	4 (44.4)	220 (73.8)	
Neoadjuvant and adjuvant	0 (0)	12 (4.0)	
No treatment	3 (33.3)	48 (16.1)	

Figure 1 - 865

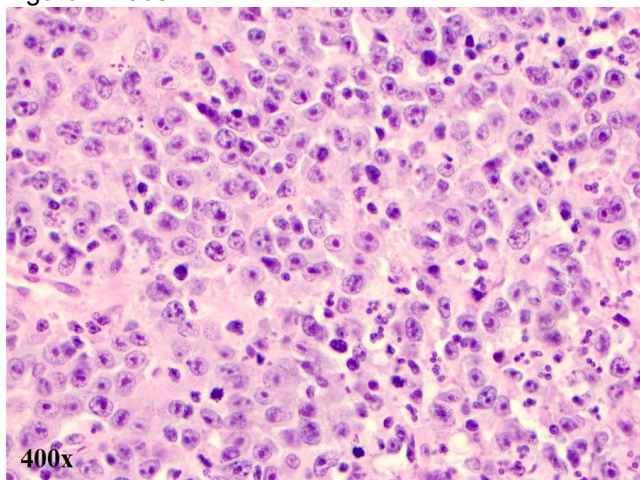
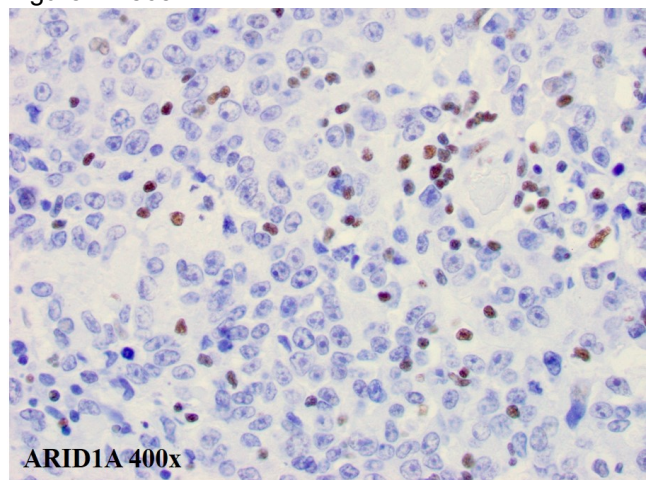


Figure 2 - 865





**Conclusions:** In this cohort, SWI/SNF deficiency was seen in 3.7% of PDAC, the vast majority of which were deficient in ARID1A. SWI/SNF deficiency is associated with older age and higher histologic grade, but did not reveal a significant association with prognosis in this aggressive cancer.

**866 Diagnosis of Metastases to the Pancreas on Small Biopsies: A Diagnostic Challenge**

Yevgen Chornenkyy<sup>1</sup>, Rebecca Obeng<sup>1</sup>, Wei Zheng<sup>2</sup>, Maryam Shirazi<sup>3</sup>, N. Volkan Adsay<sup>4</sup>, Michelle Reid<sup>5</sup>, Guang-Yu Yang<sup>6</sup>, Yue Xue<sup>1</sup>

<sup>1</sup>Northwestern University Feinberg School of Medicine, Chicago, IL, <sup>2</sup>Emory University, Atlanta, GA, <sup>3</sup>Chicago, IL, <sup>4</sup>Koç University Hospital, Istanbul, Turkey, <sup>5</sup>Emory University Hospital, Atlanta, GA, <sup>6</sup>Northwestern University, Chicago, IL

**Disclosures:** Yevgen Chornenkyy: None; Rebecca Obeng: None; Wei Zheng: None; Maryam Shirazi: None; N. Volkan Adsay: None; Michelle Reid: None; Guang-Yu Yang: None; Yue Xue: None

**Background:** Metastases to the pancreas are uncommon. Accurate identification of isolated pancreatic metastases is critical for appropriate surgical and/or medical management.

**Design:** 428 pancreatic biopsies (2015 to 2019) were reviewed to identify tumors representing metastases or secondary pancreatic involvement.

**Results:** 22 biopsies were diagnosed as metastases to pancreas. These were predominantly epithelial, most frequently from lung (n=3) and kidney (n=3), followed by breast (n=2), skin (Merkel cell carcinoma [MCC]) (n=2), ovary (n=2), prostate (n=1), head&neck (n=1), and small bowel (n=1). There were 7 non-epithelial malignancies including 4 hematopoietic, 2 leiomyosarcomas and 1 hemangiopericytoma. Interval from initial diagnosis to metastasis ranged from simultaneous diagnosis to 17 yrs), but >50% (n=12/22) were between 2 and 13 years, with lung and breast metastases occurring >10 years after primary diagnosis. Symptoms were mostly nonspecific; abdominal pain was most common (n=10/14). Tumors were mostly single (n=16/22) and 60% (n=12/19) were misdiagnosed radiologically as primaries. Morphologically lung (Fig 1a) and breast adenocarcinoma (Fig 1b) resembled pancreatobiliary-type pancreatic ductal adenocarcinoma and even well-differentiated neuroendocrine tumor (WDNET) (n=1) (Fig 1c). Lymphoma and myeloid sarcoma mimicked pancreatic neuroendocrine carcinoma (PanNEC) and had extensive crushed artifact (fig 1d). One MCC was misdiagnosed as PanNEC (Fig 1e). A prostatic NEC and an ileal WDNET were almost misdiagnosed as primaries until history of previous malignancy was obtained.

Figure 1 - 866

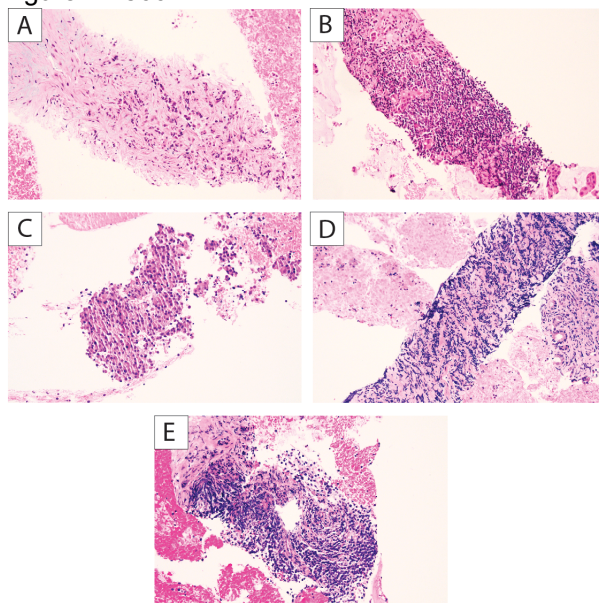


Figure 1 - Metastatic tumor mimicks primary pancreatic neoplasm.

**Conclusions:** Secondary tumors constituted ~5% of pancreatic biopsies. The majority are epithelial, followed by lymphoma. These may cause difficulties in differential diagnosis from primary pancreatic cancers, particularly in those with remote cancer history, since they form solitary tumors that closely resemble pancreatic primaries on small biopsies. Secondary tumors of the pancreas ought to be considered in the differential diagnosis of pancreatic lesions in patients with a history of a malignant tumor.

### **867 PAXgene Fixation for Pancreatic Cancer: Implications for Molecular and Diagnostic Surgical Pathology**

Ryan DeCoste<sup>1</sup>, Sarah Nersesian<sup>2</sup>, Lauren Westhaver<sup>2</sup>, Stacey Lee<sup>2</sup>, Michael Carter<sup>3</sup>, Heidi Sapp<sup>2</sup>, Ashley Stueck<sup>2</sup>, Thomas Arnason<sup>2</sup>, Jeanette Boudreau<sup>2</sup>, Weei-Yuarn Huang<sup>4</sup>

<sup>1</sup>Queen Elizabeth II Health Sciences Centre, Halifax, Canada, <sup>2</sup>Dalhousie University, Halifax, Canada, <sup>3</sup>NSHA, Halifax, Canada, <sup>4</sup>Sunnybrook Health Sciences Centre, Toronto, Canada

**Disclosures:** Ryan DeCoste: None; Sarah Nersesian: None; Lauren Westhaver: None; Stacey Lee: None; Michael Carter: None; Heidi Sapp: None; Ashley Stueck: None; Jeanette Boudreau: None; Weei-Yuarn Huang: None

**Background:** Comprehensive genomic profiling of unresectable pancreatic cancer using core biopsies has taken an increasingly prominent role in precision medicine. However, if not appropriately preserved, nucleic acids (NA) from pancreatic tissues are susceptible to degradation due to high intrinsic levels of nucleases. PAXgene fixation (PreAnalytix, Hombrechtikon, Switzerland) is a novel formalin-free tissue preservation method. We sought to compare the NA and histologic preservation of pancreatic cancer tissue samples preserved with PAXgene-fixed paraffin-embedding (PFPE) and formalin-fixed paraffin-embedding (FFPE), the current standard for laboratory tissue preservation due to favorable histomorphology.

**Design:** Tissue was obtained prospectively from pancreaticoduodenectomy specimens in accordance with local tumor banking protocols (Sept 2018–Oct 2019). We punched two representative tumor cores from each specimen. One core was fixed in formalin, and the other in PAXgene. H&E-stained slides of each core were obtained following tissue processing. Blinded evaluation of histology was performed by four gastrointestinal pathologists. NA was extracted from the remaining tissue cores, quantified by Nanodrop and assessed for quality by qPCR and agarose gel. Data were analyzed using descriptive statistics.

**Results:** Samples were obtained from 19 cases. Between four pathologists, 52.6% of H&E-stained slides were correctly identified as deriving from FFPE, and 55.3% of slides were correctly identified as deriving from PFPE (P=0.87). When assessed blindly for morphological quality, all PFPE slides were deemed adequate for diagnostic purposes. DNA extraction yielded 118.6 ng/uL and 144.4 ng/uL for FFPE and PFPE samples (P=0.56). RNA extraction yielded 73.2 ng/uL and 109.3 ng/uL for FFPE and PFPE samples (P=0.057). By qPCR, PFPE tissues consistently contained 4-fold more amplifiable DNA compared to paired FFPE samples (P<0.01). There was no significant difference in amplifiable RNA.

**Conclusions:** PFPE tissue yielded H&E-stained sections that were morphologically acceptable for diagnostic purposes. Pathologists only correctly distinguished slides as deriving from FFPE or PFPE just over half of the time, demonstrating comparable histomorphologic quality of FFPE and PFPE tissues. More amplifiable DNA was present in PFPE samples, suggesting better preservation of DNA compared to FFPE samples. Our results support the use of PAXgene fixative for the processing of biopsies from pancreatic cancers.

### **868 Comparison of the 7th and the 8th Editions of the American Joint Committee on Cancer Staging Systems for Ampulla of Vater Carcinoma**

Haijuan Gao<sup>1</sup>, Vishal Chandan<sup>1</sup>, Cary Johnson<sup>2</sup>, Yunxia Lu<sup>3</sup>, Xiaodong Li<sup>4</sup>

<sup>1</sup>University of California, Irvine, Orange, CA, <sup>2</sup>University of California, Irvine, Irvine, CA, <sup>3</sup>Irvine, CA, <sup>4</sup>UCI Medical Center, South Pasadena, CA

**Disclosures:** Haijuan Gao: None; Vishal Chandan: None; Cary Johnson: None; Yunxia Lu: None; Xiaodong Li: None



**Background:** The 8<sup>th</sup> edition of the AJCC staging system employs a more stratified T and N staging criteria for Ampulla of Vater carcinoma. How accurately these new staging systems correlate with patient prognosis haven't been well examined (PMID: 29452703). The aim of this study was to compare the 7<sup>th</sup> and 8<sup>th</sup> AJCC staging systems for ampullary carcinoma with patient prognosis.

**Design:** 66 cases of ampullary carcinoma with Whipple resections from January 2006 to December 2017 were retrieved from a tertiary academic center. The cases were re-staged using both the 7<sup>th</sup> and 8<sup>th</sup> AJCC systems. Clinical outcomes with respect to T and N stages were correlated.

**Results:** Mean age 66 years (range: 31-86), M/F: 2.14. 31(47%) tumors were intra-ampullary, 11(16.6%) peri-ampullary, and 24(36.4%) mixed type. On histology, 41(62.1%) cases were pancreaticobiliary, 20(30.3%) intestinal, 3(4.5%) mucinous, 1(1.5%) carcinosarcoma and 1(1.5%) signet ring cell. Tumor size ranged from 0.36 to 7 cm. Perineural invasion (PNI) and lymphovascular invasion (LVI) identified in 47(71.2%) and 44(66.7%) cases. 9 cases had positive margin. Patient follow-up ranged from 1.5 to 120 months. An equal number of cases in both 7<sup>th</sup> and 8<sup>th</sup> systems were pTis (1/1.5%), pT1 (5/7.5%), and pT2 (13/19.7%). Of note, in 8<sup>th</sup> AJCC, the 5 pT1 cases were further divided into T1a (3) and T1b (2). Also, in 8<sup>th</sup> AJCC all of the 7<sup>th</sup> AJCC T4 cases (33) were grouped into pT3b stage. The 3-year survival by 7<sup>th</sup> edition: T3 (9.8%) is not significantly different from T4 (33.3%) ( $p=0.128$ ); however with 8<sup>th</sup> edition: the difference between T3a (75.0%) and T3b (33.3%) is significant ( $p=0.029$ ). Furthermore, higher rates of PNI, LVI, and margin positivity present in the T3b in comparison to pT3a tumor groups ( $p < 0.001$ ) within 8<sup>th</sup> AJCC. In the 8<sup>th</sup> edition, 45 prior N1 (positive LN $\geq$ 1) stage cases were sub-grouped into 20 N1 (positive LN $\geq$ 1) and 25N2 (positive LN $\geq$ 4) stages. Although the 7<sup>th</sup> AJCC nodal stage presents different clinical outcomes between N0 and N1 groups (Log-Rank,  $p=0.013$ ), sub-staging nodal status in the 8<sup>th</sup> edition provided a more stratified prediction of clinical outcome between N1 and N2 groups (Log-Rank,  $p=0.0235$ ).

**Conclusions:** The AJCC 8<sup>th</sup> edition with its increased stratification of T and N parameters better predicts patient prognosis, especially the new nodal staging criteria.

### **869 Detection of Gallbladder Carcinomas and Other Unforeseen Findings on Pathological Evaluation of 1553 Gallbladder Specimens: An Institutional Review Over a Five-Year Period**

Alan George<sup>1</sup>, Clara Milikowski<sup>2</sup>, Elizabeth Montgomery<sup>3</sup>, Maryam Tahir<sup>3</sup>, Parthavkumar Patel<sup>1</sup>, Julio Poveda<sup>3</sup>, Jonathan England<sup>3</sup>, Nemencio Ronquillo<sup>1</sup>, Monica Garcia-Buitrago<sup>4</sup>

<sup>1</sup>Jackson Memorial Hospital/University of Miami Hospital, Miami, FL, <sup>2</sup>University of Miami/Jackson Memorial Hospital, Miami, FL, <sup>3</sup>University of Miami Miller School of Medicine, Miami, FL, <sup>4</sup>University of Miami Miller School of Medicine/Jackson Health System, Miami, FL

**Disclosures:** Alan George: None; Clara Milikowski: None; Elizabeth Montgomery: None; Maryam Tahir: None; Parthavkumar Patel: None; Julio Poveda: None; Jonathan England: None; Nemencio Ronquillo: None; Monica Garcia-Buitrago: None

**Background:** Gallbladders with "incidental" or unexpected carcinomas have been estimated to account for 0.23%-1.5% of cholecystectomy specimens removed for presumed benign gallbladder disease. The general consensus seems to indicate that routine histopathologic evaluation of cholecystectomies is of value, given the possibility of detecting unexpected malignancy; however, alternative practices have been suggested in certain clinical scenarios such as on-table evaluation of specimens by surgeons intraoperatively for concerning lesions. In this study, we determined the incidence of unexpected findings in gallbladder specimens resected at our institution, including malignancy and dysplasia, as well as benign polyps/polypoid lesions.

**Design:** The pathology database of our large urban Southeast United States teaching hospital system was queried for gallbladder resections from 2015 - 2020. The pathology reports and pertinent clinical notes were reviewed.

**Results:** A total of 1553 cholecystectomies (62.4% females, 37.6% males; median age 55) were performed and histologically evaluated during this period, the majority of which showed expected gallbladder disease, including cholecystitis (1419, 91.4%) and cholelithiasis (1087, 70%). Adenomyomas were identified in 20 cases (1.3%) and other benign polyps were found in 67 cases (4.3%). Twelve invasive gallbladder carcinomas were identified (0.77%), in 9 women and 3 men (median age 70). Of these 12 carcinomas, 7 (58%) were occult, and 5 (42%) were

clinically suspected. Therefore the frequency of occult gallbladder carcinomas at our institution was 0.5%. Additional neoplastic lesions included well-differentiated neuroendocrine tumor (1, 0.06%), intracholecystic papillary neoplasm/pyloric gland adenomas (5, 0.3%), as well as biliary intraepithelial neoplasia (low grade: 8, 0.5%; high grade: 9, 0.6%). Interestingly, metastatic lesions to the gallbladder were identified in 13 cases (0.8%), though these were in patients with a known clinical history of malignancy. The 13 cases of metastatic disease are comprised of: 6 colon adenocarcinomas (46.2%), 2 ovarian serous carcinomas (15.4%), 1 renal cell carcinoma (7.7%), 1 low grade appendiceal mucinous neoplasm (7.7%), 1 yolk sac tumor (7.7%), 1 angiosarcoma (7.7%), 1 mesothelioma (7.7%).

**Conclusions:** Occult gallbladder adenocarcinomas are uncommon in cholecystectomy specimens, but worth identifying. Although the frequency of unexpected gallbladder carcinomas is around 1%, macroscopic and histological evaluation of these specimens is warranted. Additionally, we report the incidence of other unexpected gallbladder lesions at our institution, including premalignant lesions: dysplasia / intracholecystic papillary neoplasm (1.4%) and metastatic tumors that might potentially upstage the patient if gallbladder is the only metastatic site.

**870 An International Retrospective Cohort Analysis of Pancreatic Ductal Adenocarcinoma Treated With Neoadjuvant Therapy: Validation of the AJCC 8th Staging System and Tumor Response Scoring System**

Jingjing Hu<sup>1</sup>, Debashis Sahoo<sup>2</sup>, Mitchell Zhao<sup>1</sup>, Mrinal Sarwate<sup>3</sup>, Haiyan Lu<sup>4</sup>, Goo Lee<sup>5</sup>, Deepti Dhall<sup>6</sup>, Kevin Hale<sup>6</sup>, Yoko Matsuda<sup>7</sup>, Yasuyuki Suzuki<sup>7</sup>, Keiichi Okano<sup>7</sup>, Jiaqi Shi<sup>8</sup>, Jiayun Fang<sup>9</sup>, William Perry<sup>10</sup>, Vikram Deshpande<sup>11</sup>, Amaya Pankaj<sup>12</sup>, Irene Esposito<sup>13</sup>, Lena Haeberle<sup>14</sup>, Rebekah White<sup>2</sup>, Andrew Lowy<sup>2</sup>, Daniela Allende<sup>15</sup>, Mojgan Hosseini-Varnamkhasti<sup>2</sup>

<sup>1</sup>University of California, San Diego, San Diego, CA, <sup>2</sup>University of California, San Diego, La Jolla, CA, <sup>3</sup>Cleveland Clinic Foundation, Cleveland, OH, <sup>4</sup>Cleveland Clinic, Cleveland, OH, <sup>5</sup>UAB Hospital, Birmingham, AL, <sup>6</sup>The University of Alabama at Birmingham, Birmingham, AL, <sup>7</sup>Kagawa University, Faculty of Medicine, Kita-gun, Japan, <sup>8</sup>University of Michigan, Ann Arbor, MI, <sup>9</sup>University of Michigan Hospitals, Ann Arbor, MI, <sup>10</sup>Michigan Medicine, University of Michigan, Ann Arbor, MI, <sup>11</sup>Massachusetts General Hospital, Harvard Medical School, Boston, MA, <sup>12</sup>Massachusetts General Hospital, Boston, MA, <sup>13</sup>Heinrich-Heine University and University Hospital of Duesseldorf, Erlangen, Germany, <sup>14</sup>Heinrich-Heine University and University Hospital of Duesseldorf, Duesseldorf, Germany, <sup>15</sup>Cleveland Clinic, Lerner College of Medicine of Case Western University School of Medicine, Cleveland, OH

**Disclosures:** Jingjing Hu: None; Debashis Sahoo: None; Mitchell Zhao: None; Mrinal Sarwate: None; Haiyan Lu: None; Goo Lee: None; Deepti Dhall: None; Yoko Matsuda: None; Yasuyuki Suzuki: None; Jiaqi Shi: None; Jiayun Fang: None; Vikram Deshpande: None; Amaya Pankaj: None; Irene Esposito: None; Lena Haeberle: None; Daniela Allende: None; Mojgan Hosseini-Varnamkhasti: None

**Background:** Pancreatic ductal adenocarcinoma (PDAC) is an aggressive neoplasm typically presenting at an advanced stage. Surgical resection is the mainstay of therapy. In recent years, neoadjuvant chemotherapy (NAC), with or without radiation, has been increasingly employed prior to surgical resection. However, staging and assessment of treatment response is particularly challenging in PDAC treated with NAC due to the presence of extensive fibrosis (due to chemotherapy, chronic pancreatitis, desmoplastic response or a combination of the three), presence of multiple and discontinuous viable tumor foci that engenders confusion as to how size should be measured for staging. Herein, we evaluated the CAP/AJCC 8th staging system and treatment response scoring system for their prognostic value in PDAC patients undergoing NAC followed by resection.

**Design:** This multicenter cohort study included multiple US and international medical institutions. The pathology databases were searched for specimens procured from resected PDAC in which NAC was delivered from 2015-2020. Clinical and pathologic data was collected from electronic medical records and pathology reports. All cases were staged using AJCC 7th and 8th editions and most recent CAP synoptic criteria. Cox proportional hazard regression and Kaplan-Meier plots were used in evaluation of the data.

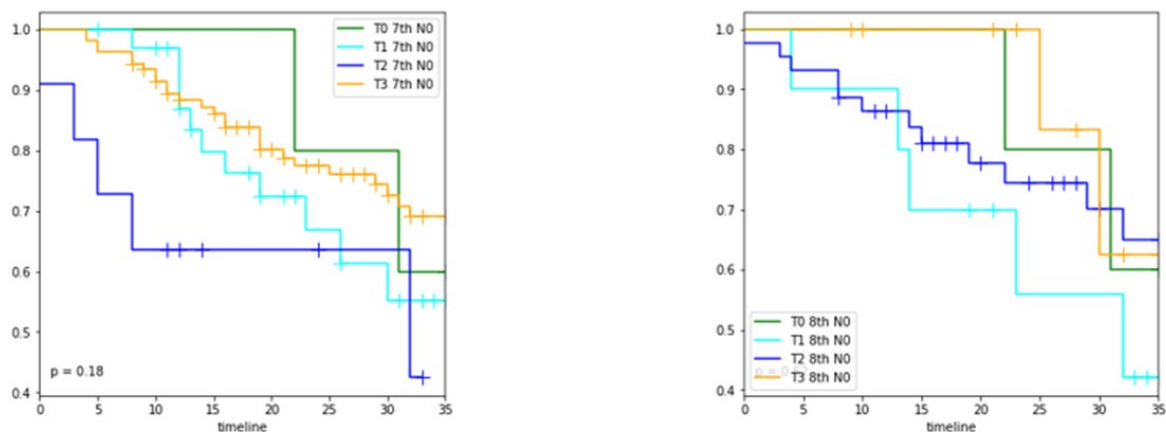
**Results:** A total of 374 cases of NAC PDAC were retrospectively analyzed and staged based on AJCC 7th and 8th editions. The clinicopathologic features were summarized in Table 1. Neither AJCC staging criteria, 7th or 8th edition, was prognostic for survival according to tumor stage, overall, or in N0 cases only (See Fig. 1). Further, no survival difference was noted when extrapancreatic extension was taken into account, stage for stage. Size of the



largest tumor focus measured microscopically ( $\leq 2\text{cm}$ ,  $p=0.037$ ) and size of the tumor bed measured grossly ( $\leq 3\text{ cm}$ ,  $p=0.018$ ) were found to be predictive of overall survival. CAP methodology of scoring treatment response also failed to stratify patient survival. Degree of post-treatment tumor differentiation, however, was predictive ( $p=0.00096$ ). Presence of positive lymph nodes was associated with worse survival, however, there was no survival difference between N1 and N2 stage.

Clinical pathologic characteristics of the entire patient cohort	
	All patients (n=374) (%)
Age, median, y	67 (30-86)
Male	218(58%)
Female	156 (42%)
Dead	135 (36%)
Margin status	
Margin negative	298 (80%)
Margin positive	76 (20%)
Harvest lymph nodes, median	18 (1-55)
Positive lymph nodes number, median	1 (0-13)
Cases with negative lymph nodes	173 (46%)
Treatment naive tumor size maximum dimension, median, cm	2.65 (0.5-9.2)
Tumor location	
Head	276 (74%)
Body or tail	93 (25%)
N/A	5 (1%)
Extrapancreatic extension	295 (79%)
Tumor differentiation (post treatment)765	
Well (G1)	75 (20%)
Moderately (G2)	170 (45%)
Poorly (G3)	85 (23%)
unknown	44 (12%)
Perineural invasion	
Present	282 (75%)
Absent	91 (24%)
Lymphovascular invasion	
Present	195 (52%)
Absent	167 (45%)
Indeterminate	10 (3%)

Figure 1 - 870



**Conclusions:** Staging and assessment of post neoadjuvant residual tumor burden is critical for predicting tumor prognosis in various malignancies. However the current size based staging and subjective evaluation of residual tumor burden fail to be accurate or prognostic in PDAC treated with NAC. Staging NAC treated tumor and assessing treatment response needs better defined criteria with objective parameters that could be easily applied. The current data suggests the need for a modified staging system for PDAC treated with NAC and that cut offs of 2 cm for tumor focus and 3 cm for tumor bed appear to be prognostic for survival.

**871 Diagnostic Value of DNA-Based Molecular Analysis of Cyst Fluid for Risk Stratification of Pancreatic Cystic Lesions**

Charmaine Ilagan<sup>1</sup>, Emily Winslow<sup>1</sup>, Walid Chalhoub<sup>1</sup>, Michelle Xu<sup>1</sup>, Jae Sung<sup>1</sup>, Mary Sidawy<sup>1</sup>  
<sup>1</sup>MedStar Georgetown University Hospital, Washington, DC

**Disclosures:** Charmaine Ilagan: None; Emily Winslow: None; Walid Chalhoub: None; Michelle Xu: None; Jae Sung: None; Mary Sidawy: None

**Background:** The incidence of pancreatic cysts has increased with advancement in imaging. Pancreatic cysts carry various risks of malignancy. As management is evolving from surgery to surveillance, there is a need for better predictors of malignant potential. Endoscopic ultrasound-guided fine needle aspiration (EUS-FNA) is associated with a significant nondiagnostic rate. Molecular analysis of the fluid has emerged as an ancillary tool and a potential predictor. The purpose of this study is to evaluate the value of molecular analysis in stratifying the risk of malignancy in pancreatic cyst fluid.

**Design:** We retrospectively searched our database (2012-19) for patients who underwent molecular analysis of pancreatic cyst fluid by PancreaGEN®. Patients with EUS-FNA and surgical pathology follow-up (F/U) were included in the study. PancreaGEN® is a DNA-based, integrated molecular test that assesses the risk of cancer in pancreatic cysts using an algorithm that includes clinical features and molecular alterations. Biological behavior is classified as benign, statistically indolent, statistically higher risk, aggressive and indeterminate. The molecular classification was correlated with surgical pathology F/U. FNA results (diagnostic vs. nondiagnostic) and CEA levels were also evaluated for a subgroup that included invasive carcinomas, intraductal papillary mucinous neoplasms (IPMN), mucinous cystic neoplasms (MCN), and pancreatic intraepithelial neoplasia (PanIN).

**Results:** 67/572 patients were included in the study (24 men, 43 women), age range of 31-86 years (mean: 64). Table 1 summarizes the correlation of the molecular classification with surgical pathology F/U. 58/67 cases were invasive carcinoma, IPMN, MCN and PanIN (45/58 low grade, 13 high grade/malignant). The remaining 9 were miscellaneous lesions. 37/45 (82%) low grade lesions (32 IPMN, 12 MCN, 1 PANIN-1) were classified as benign or statistically indolent, while 6/13 (46%) high grade/malignant lesions (2 IPMN, 11 invasive carcinoma) were classified as statistically higher risk. In comparison, FNAs were diagnostic in 12/45 (27%) low grade lesions, and 7/13 (54%) high grade/malignant lesions. CEA was ≥192 ng/mL in 45/58 (78%).

Table 1:

Surgical Pathology F/U	Molecular Risk Stratification of Pancreatic Cyst Fluid					Total
	Benign	Statistically Indolent	Statistically higher risk	Aggressive	Indeterminate	
IPMN, low grade	13	12	7			32
IPMN, high grade	1		1			2
MCN, low grade	8	3	1			12
Pancreatitis with PanIN-1	1					1
Invasive Carcinoma	4	1	5		1	11
Miscellaneous*	9					9
<b>Total</b>	<b>36</b>	<b>16</b>	<b>14</b>		<b>1</b>	<b>67</b>

\*Miscellaneous (9 cases) all classified as Benign: Neuroendocrine tumor (2), serous cystadenoma (2), solid pseudopapillary neoplasm (1), cystic lymphangioma (1), pancreatitis with ectatic duct (1), pseudocyst (1), accessory splenic cyst (1).

**Conclusions:** Our study demonstrated that molecular analysis is useful in stratifying the risk of malignancy in pancreatic cysts but is not an absolute predictor. Multiple diagnostic modalities to include cytology, CEA and molecular analyses, along with clinical characteristics, are necessary to guide patient management.

**872 Challenges in the Classification of High-Grade Neuroendocrine Neoplasms Based on Current Recommendations**

Nancy Joseph<sup>1</sup>, Grace Kim<sup>1</sup>, Sarah Umetsu<sup>1</sup>, Sanjay Kakar<sup>1</sup>

<sup>1</sup>University of California, San Francisco, San Francisco, CA

**Disclosures:** Nancy Joseph: None; Grace Kim: None; Sarah Umetsu: None; Sanjay Kakar: None

**Background:** Grade 3 neuroendocrine tumor (G3 NET) and neuroendocrine carcinoma (NEC) are both defined by Ki67 >20% and/or mitoses >20 per 2mm<sup>2</sup>. NET and NEC are thought to be distinct tumors with distinct genetics, and progression from NET to NEC is considered rare. *MEN1*, *ATRX*, and *DAXX* mutations are considered typical of NET, while *TP53* and *RB1* mutations are typical of NEC and immunostains for ATRX/DAXX/p53/Rb are recommended in the classification of G3 NET versus NEC. It is also recommended that a high-grade neuroendocrine neoplasm (NEN) should be classified as G3 NET in the presence of a lower grade NET component irrespective of morphology (PMID: 27259015, 33002892). We have earlier described co-occurrence of *MEN1* and *TP53* alterations in G3 NET (abstract). This small series highlights additional challenges in classification of NENs based on current recommendations.

**Design:** Challenging high-grade neuroendocrine cases from our archives and consult service were reviewed by four expert pathologists. The cases were evaluated based on WHO 2019 classification. Immunohistochemistry for Rb, p53 and p16 was performed, and Ki-67 proliferation index was determined semi-quantitatively by counting at least 500 tumor cells.

**Results:** This series comprises 4 high-grade NENs. Progression from a G1, G2, or G3 NET to a neoplasm indistinguishable from NEC was seen in 3 cases. Of these, progression in 1 case was seen within the same biopsy of G1 NET to a NEC-like morphology and was accompanied by Rb loss only in the NEC component. In the other 2 cases, progression from a prior G2 or G3 NET to a recurrence with NEC-like morphology was seen 3 to 12 years later. Co-occurrence of mutations in *MEN1*, *ATRX*, *TP53*, and *RB1* was seen in one case and the other had co-occurrence of *MEN1* and *TP53*. The fourth case demonstrated G3 NET morphology, but showed loss of Rb; morphologic features of NEC were not present.

High-grade NEN cases that demonstrate challenges in classification

Case	Age/sex	Primary site, procedure	Metastasis/recurrence, procedure after time interval	Morphologic features of primary and/or metastasis/recurrence	Ki67 of progression	Immunohistochemical/Genomic features
1	37/M	Sacrum, biopsy	Liver metastasis biopsy, 3 years later	Primary tumor and liver metastasis are predominantly G1 NET with foci showing morphologic features of NEC in the primary tumor	70%	Rb loss and diffuse p16 only in NEC-like component. No NGS
2	58/M	Pancreas, resection	Liver metastasis biopsy, 12 years later	Pancreas shows G2 NET morphology; liver metastasis shows morphologic features of NEC	75%	Rb loss, NGS shows <i>MEN1</i> , <i>ATRX</i> , <i>TP53</i> and <i>RB1</i> mutations, not hypermutated
3	29/F	Unknown; liver metastasis resection	Liver recurrence biopsy, 3 years later	Liver metastasis shows G3 NET morphology; recurrence shows morphologic features of NEC	>95%	Rb intact, NGS shows <i>MEN1</i> and <i>TP53</i> mutations in both original and recurrent liver metastasis; but equivocal CCNE in recurrence. MSI-high in both
4	58/M	Pancreas, not biopsied	Liver metastasis biopsy	Liver metastasis has NET morphology, no morphologic features of NEC	34%	Rb loss, diffuse p16. No NGS

**Conclusions:** These cases show that NET can progress to a neoplasm that is morphologically indistinguishable from NEC and genetically harbors mutations in *TP53* and/or *RB1*. Also, neoplasms with NET morphology can show Rb loss. Further studies are needed to determine the frequency of these occurrences and clinical outcomes in these cases. These cases raise questions about the currently used criteria and recommendations for the classification of G3 NET versus NEC as there appears to be more immunohistochemical and genetic overlap than previously appreciated.



**873 Spatial Immunoarchitectural Intra-Tumor Heterogeneity is Associated with Early Tumor Recurrence in Pancreatic Cancer**

Eva Karamitopoulou-Diamantis<sup>1</sup>, Andreas Andreou<sup>2</sup>, Aurel Perren<sup>3</sup>, Beat Gloor<sup>2</sup>

<sup>1</sup>Institute of Pathology, University of Bern, Bern, Switzerland, <sup>2</sup>Insel University Hospital, University of Bern, Bern, Switzerland, <sup>3</sup>University of Bern, Bern, Switzerland

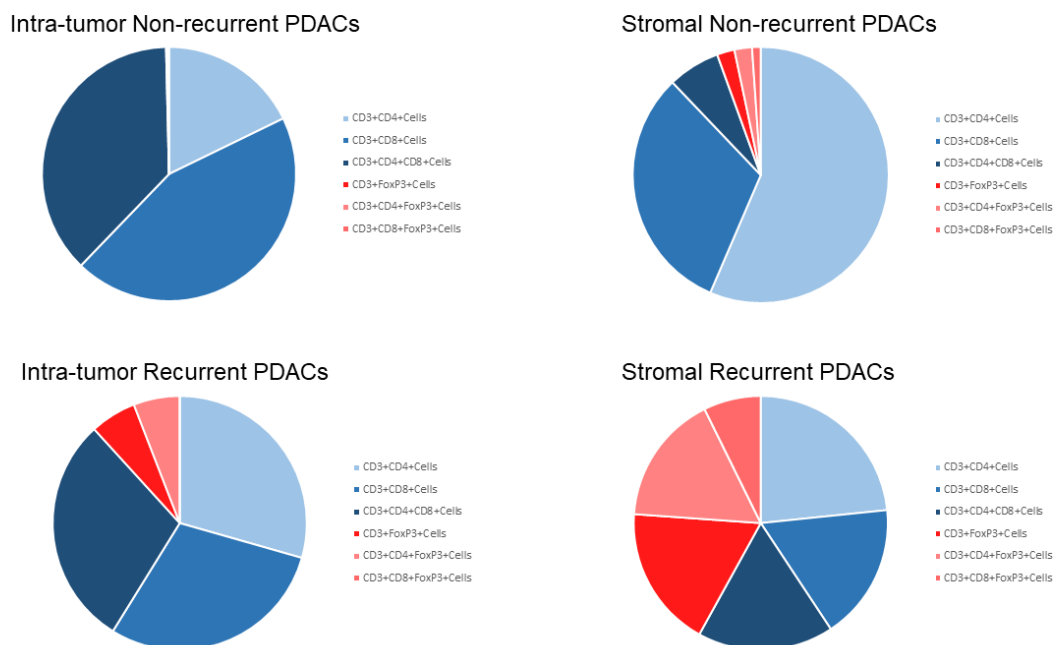
**Disclosures:** Eva Karamitopoulou-Diamantis: None; Aurel Perren: None

**Background:** Intra-tumor heterogeneity (ITH) is known to correlate with tumor progression and poor outcomes. The impact of ITH in early recurrence of pancreatic ductal adenocarcinoma (PDAC) has not yet been adequately addressed.

**Design:** Thirty PDACs stage IIB, including 15 cases with early recurrence (<12 months after resection) and 15 without recurrence >36 months after resection were histomorphologically assessed for gland-forming component (G1-3), tumor budding (Bd1-3) and percentage of solid growth (So1-3). Cases were stained by multiplex immunofluorescence for CD3, CD4, CD8, FOXP3 and CD68, followed by morphometric and proximity analysis of each three, morphologically different, regions of interest (ROIs, n:90) and were genetically analyzed by using the oncoPrint comprehensive assay V3. Results were validated in a bigger cohort (n=110).

**Results:** Non-recurrent PDACs exhibited histomorphologic uniformity with extensive gland-forming component (G13). A microenvironment rich in cytotoxic CD3<sup>+</sup>/CD8<sup>+</sup>T cells and CD3<sup>+</sup>/CD4<sup>+</sup>T-helper cells in close proximity to tumor cells (average 20µm), but poor in CD3<sup>+</sup>/FOXP3<sup>+</sup> regulatory cells, with some quantitative differences among ROIs, was present. In contrast, recurrent cases exhibited significant histomorphologic heterogeneity with alternate areas of high-grade tumor budding (Bd3) and solid growth (So2-3) adjacent to gland-forming component (G11,2). Their microenvironment showed significant quantitative and qualitative regional variability. In some ROIs CD68<sup>+</sup>macrophages predominated, while in ROIs with higher T cell counts an increased proportion of the CD3<sup>+</sup> and/or CD4<sup>+</sup>T cells co-expressed FOXP3, as compared with the non-recurrent cases (p<0.001). The average distance of CD8<sup>+</sup>T cells to tumor cells was 40µm (p<0.001). Significant inter- but not intra-tumor genetic heterogeneity was noted. High concordance regarding histomorphologic findings was observed between study and validation cohort. Increased numbers of CD3<sup>+</sup>, CD4<sup>+</sup> and CD8<sup>+</sup>T cells correlated with longer progression-free survival in the validation cohort.

Figure 1 - 873



**Conclusions:** Early recurrence in PDAC is associated with significant spatial histomorphologic and immunoarchitectural heterogeneity. This suggests spatial interactions between cancer- and immune cells with regional differences in recruitment of immune responses, which by locally changing the balance between anti- and pro-tumorigenic factors create different selection pressures to guide tumor progression.

**874 Immunoarchitectural Features of PD-1/PD-L1-Mediated Immune Resistance Stratify Pancreatic Cancer Patients into Prognostic/Predictive Subgroups**

Eva Karamitopoulou-Diamantis<sup>1</sup>, Aurélie Pahud de Mortanges<sup>2</sup>, Andreas Andreou<sup>3</sup>, Marianne Tinguely<sup>4</sup>, Aurel Perren<sup>2</sup>, Beat Gloor<sup>3</sup>

<sup>1</sup>Institute of Pathology, University of Bern, Bern, Switzerland, <sup>2</sup>University of Bern, Bern, Switzerland, <sup>3</sup>Insel University Hospital, University of Bern, Bern, Switzerland, <sup>4</sup>Zurich, Switzerland

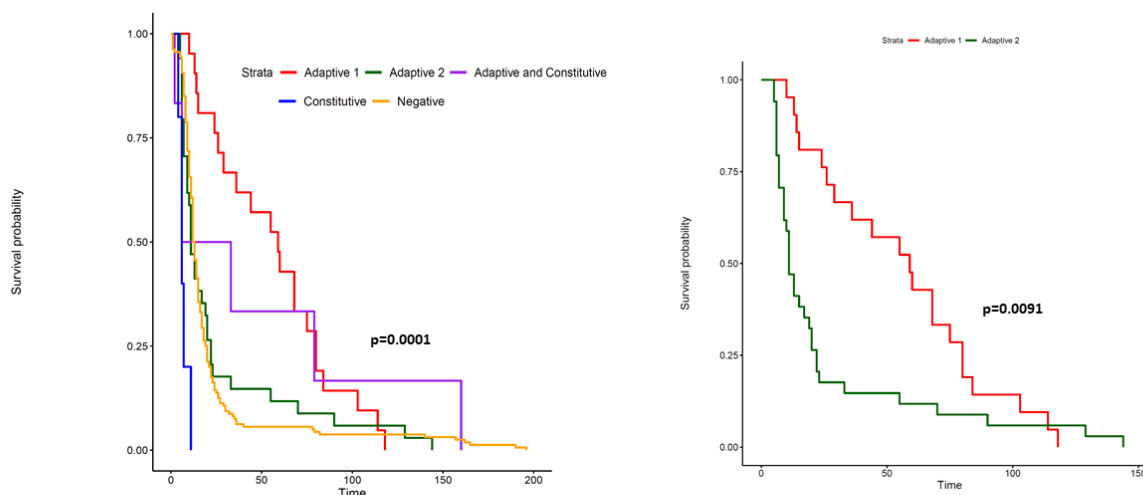
**Disclosures:** Eva Karamitopoulou-Diamantis: None; Aurélie Pahud de Mortanges: None

**Background:** Immunotherapy, including PD-1/PD-L1 antagonists, has shown limited activity for patients with pancreatic ductal adenocarcinoma (PDAC). Improved biomarker assessment will help identifying patients most likely to respond thereby increasing the success of immune-based therapies.

**Design:** 112 PDACs were evaluated for PD-L1-expression by immunohistochemistry on tissue microarrays. Whole-tissue sections of PD-L1<sup>+</sup>cases were further examined by multiplex immunofluorescence (PD-1, PD-L1, CD3, CD4, CD8, FOXP3, CD68) followed by morphometric analysis of the immunoarchitectural features. Results were validated in a parallel cohort (n=226).

**Results:** PD-L1-expression in >1% of the tumor cells (TC) and/or immune cells (IC) was seen in 33% of PDACs of the study cohort and 30% of the cases of the validation cohort and was assigned to one of 4 patterns: *Adaptive 1*: PD-L1<sup>+</sup>IC>1%, PD-L1<sup>+</sup>TC=0; *Adaptive 2*: PD-L1<sup>+</sup>IC>1%, PD-L1<sup>+</sup>TC=>1%; *Constitutive/Innate*: PD-L1<sup>+</sup>IC=0, PD-L1<sup>+</sup>TC>50% and *Combined*: PD-L1<sup>+</sup>TC>50%, PD-L1<sup>+</sup>IC>1%. The immunoarchitectural characteristics of the tumor microenvironment differed significantly among the different patterns. *Adaptive 1* (32% of the PD-L1<sup>+</sup>PDACs) phenotype was associated with a “hot” microenvironment displaying increased counts of cytotoxic CD3<sup>+</sup>/CD8<sup>+</sup>Tcells, a small percentage of which exhibited exhausted (CD8<sup>+</sup>/PD-1<sup>+</sup>) or immunosuppressive (CD8<sup>+</sup>/PD-L1<sup>+</sup>) phenotypes. Patients with *Adaptive 1* phenotype had longer overall survival (p=0.001). *Adaptive 2* (49% of the PD-L1<sup>+</sup>cases) was associated with increased counts of immunosuppressive CD8<sup>+</sup>/PD-L1<sup>+</sup>T cells and immune-evading TC, while the less frequent constitutive pattern (11% of PD-L1<sup>+</sup>cases) was invariably correlated with an immune deserted microenvironment, extensive presence of immune-evading TC and worse outcome. The presence of adaptive characteristics in the combined pattern (8% of PD-L1<sup>+</sup>PDACs) conferred survival advantage. A high concordance in the proportional distribution of the PD-1/PD-L1-associated immune resistance patterns and their correlation with outcome was observed between study and validation cohort.

Figure 1 - 874



**Conclusions:** Our findings suggest that the immunoarchitectural features in the tumor microenvironment might influence the efficacy of anti-PD-1-PD-L1 immunotherapy. PDAC-patients with *Adaptive 1* pattern might profit from treatments incorporating checkpoint inhibition. The evaluation of PD-L1 should be part of an individualized precision oncology approach in PDAC.

**875 TRAILshort is a Novel Potential Therapeutic Target in Pancreatic Ductal Adenocarcinoma**  
Binny Khandakar<sup>1</sup>, Aswath P. Chandrasekar<sup>2</sup>, Ashton Krogman<sup>2</sup>, Benjamin VanTreeck<sup>2</sup>, Nathan Cummins<sup>2</sup>, Sekar Natesampillai<sup>2</sup>, Enrique Garcia-Rivera<sup>3</sup>, Mahendra Rathore<sup>2</sup>, Khashayarsha Khazaie<sup>2</sup>, Andrew Badley<sup>2</sup>, Rondell Graham<sup>2</sup>  
<sup>1</sup>Mount Sinai St. Luke's Roosevelt Hospital, New York, NY, <sup>2</sup>Mayo Clinic, Rochester, MN, <sup>3</sup>Cambridge, MA

**Disclosures:** Binny Khandakar: None; Aswath P. Chandrasekar: None; Ashton Krogman: None; Benjamin Van Treeck: None; Nathan Cummins: None; Sekar Natesampillai: None; Enrique Garcia-Rivera: None; Mahendra Rathore: None; Khashayarsha Khazaie: None; Andrew Badley: *Stock Ownership*, Splissen Therapeutics; Rondell Graham: None

**Background:** Pancreatic ductal adenocarcinoma (PDAC) has a poor prognosis with very limited systemic treatment options. Recently, we have described a novel immune checkpoint protein, TRAILshort which is present in the microenvironment in various solid and hematologic malignancies. TRAILshort antagonizes full length TNF-related apoptosis inducing ligand (TRAIL) inhibiting its pro-apoptotic effect. We designed this study to evaluate if TRAILshort is a potential therapeutic target in PDAC.

**Design:** We evaluated publicly available, transcriptomic data from PDAC in The Cancer Genome Atlas (TCGA) for TRAILshort mRNA in PDAC and examined the corresponding patient outcome. Thereafter, we examined 9 randomly selected PDAC from our clinical practice for TRAILshort immunohistochemistry and RNA in situ hybridization. Using 3 different PDAC cell lines, we determined whether inhibiting TRAILshort in the presence of TRAIL affected cell killing. Using humanized mice with implanted PDAC (n=6), we treated 3 with anti-TRAILshort and 3 with isotype IgG. At death, the PDAC xenografts were assessed for tumor size as well as CD3 and CD8 infiltrate and apoptoses.

**Results:** Normalized data from the TCGA revealed the presence of TRAILshort mRNA in PDAC and high levels (n=45 of 185 cases) significantly corresponded with worse overall survival (p=0.034). TRAILshort protein and mRNA were detected in 5 of 9 cases of randomly selected clinical PDAC. In the cell line with TRAILshort, the addition of anti-TRAILshort in the presence of TRAIL augmented cell killing by 25% compared to controls. The 2 cell lines without TRAILshort did not show augmented cell killing. The tumors from anti-TRAILshort-treated mice were smaller than those from mice receiving control IgG (median 744.2 mm<sup>3</sup> compared to 2470 mm<sup>3</sup>), showed greater CD3 and CD8 positive T-cell infiltration (medians 227 vs 193 cells/mm<sup>2</sup>; 157 vs 142 cells/mm<sup>2</sup> respectively) and more apoptotic cells (median 183 vs 33 cells/mm<sup>2</sup>).

**Conclusions:** TRAILshort is present in the immune microenvironment in a subset of PDAC based on TCGA data and our clinical cases. High levels of TRAILshort are associated with worse prognosis in PDAC. Treatment of PDAC cell lines with TRAILshort in the immune microenvironment and PDAC xenografts with TRAIL and anti-TRAILshort antibody were associated with augmented cell killing. These data indicate that TRAILshort is potential novel predictive therapeutic biomarker in PDAC.

**876 PD-L1 Expression is Enriched in Intraductal Oncocytic Papillary Neoplasm (IOPN)**  
Anna Lee<sup>1</sup>, Ladan Fazlollahi<sup>2</sup>, Helen Remotti<sup>1</sup>  
<sup>1</sup>Columbia University Medical Center, New York, NY, <sup>2</sup>New York-Presbyterian/Columbia University Medical Center, New York, NY

**Disclosures:** Anna Lee: None; Ladan Fazlollahi: None; Helen Remotti: None

**Background:** Immune checkpoint inhibitors have been successfully used to treat a wide variety of tumors, and use of PD-L1 immunohistochemical (IHC) scoring is the currently accepted method to identify tumors that are more likely to respond to such therapies. PD-L1 expression has been shown to be low in pancreatic carcinomas. The aim



of this study was to perform a survey of PD-L1 expression in multiple pancreatic neoplasms, including pancreatic adenocarcinoma, pancreatic neuroendocrine tumor (PanNET), pancreatic neuroendocrine carcinoma (PanNEC), acinar cell carcinoma (ACC), solid pseudopapillary tumor (SPT), mucinous cystic neoplasm (MCN), acinar cystadenoma (AC), serous cystadenoma (SC), intraductal papillary mucinous neoplasm (IPMN), and intraductal oncocyctic papillary neoplasm (IOPN).

**Design:** Tissue microarrays (TMAs) were created from pancreatic neoplasms from intradepartmental archives. The tumor histologic type distribution was as follows: 20 pancreatic adenocarcinomas, 27 IPMNs (10 high grade, 17 low grade), 8 IOPNs, 54 PanNETs, 4 PanNECs, 6 SPTs, 2 ACCs, 2 MCNs, 2 ACs, and 1 SC. PD-L1 immunohistochemical staining was performed on the TMAs. Three different PD-L1 clones were tested: SP142 (Roche), 22C3 (Agilent Dako), and 73-10 (Abcam). PD-L1 expression was scored using the Combined Positive Score (CPS) methodology on each TMA core and a mean CPS score was calculated from the CPS scores for cores from the same case.

**Results:** Of the 126 cases tested, only 7 showed PD-L1 expression, all of which were IOPN cases (Table 1). All other pancreatic neoplasms tested were negative for PD-L1 staining (CPS < 1). Of the three clones tested, only 22C3 and 73-10 showed staining, with 7 cases showing CPS > 1, and of these, 5 cases showed CPS > 10. Staining patterns were similar between 22C3 and 73-10 for each core. The 8 patients in the IOPN group ranged from 41 to 83 years of age, and 5 (63%) of these cases were associated with an invasive carcinoma.

**Table 1:** IOPN cases show PD-L1 expression by immunohistochemistry

Case	Invasive component?	PD-L1 22C3 Mean CPS	PD-L1 73-10 Mean CPS
IOPN-1	Y	5.0	17.0
IOPN-2	Y	31.3	42.5
IOPN-3	Y	16.8	21.0
IOPN-4	Y	3.3	3.8
IOPN-5	N	2.6	3.4
IOPN-6	N	2.4	13.0
IOPN-7	N	0	0.4
IOPN-8	Y	9.6	13.0

**Conclusions:** A survey of PD-L1 staining in a wide range of pancreatic neoplasms shows enrichment of PD-L1 staining in IOPN. These findings were demonstrated using two different PD-L1 clones. These results suggest unique immunogenicity in IOPN compared to that of other pancreatic neoplasms, and that immunotherapy may have a role in the treatment of IOPN.

**877 A Clinicopathologic and Molecular Study of BRCA1/2-mutated Pancreatic Ductal Adenocarcinoma**

Hongjie Li<sup>1</sup>, Joanna Gibson<sup>1</sup>, Dhanpat Jain<sup>1</sup>, Karin Finberg<sup>1</sup>, Zenta Walther<sup>1</sup>, Minghao Zhong<sup>1</sup>  
<sup>1</sup>Yale School of Medicine, New Haven, CT

**Disclosures:** Hongjie Li: None; Dhanpat Jain: None; Karin Finberg: None; Zenta Walther: None; Minghao Zhong: None

**Background:** Pancreatic ductal adenocarcinoma (PDAC) with germline and/or somatic mutations of *BRCA1/2* makes up <5% of all PDAC and has recently gained increasing attention due to its high sensitivity to the poly adenosine diphosphate-ribose polymerase (PARP) inhibitor. However, *BRCA1/2*-mutated PDAC has not yet been well characterized at a clinicopathological and molecular level.

**Design:** We performed a retrospective search of 178 PDAC specimens that had been analyzed in parallel with a paired germline control specimen using the OncoPrint Comprehensive Assay NGS-based cancer panel (Thermo Fisher) by the Yale New Haven Hospital Tumor Profiling Laboratory between January 2017 and September 2020.

Data including clinical history, pathologic diagnosis, immunohistochemical and OncoPrint analysis (2 v2 and 5 v3 reports) were extracted from patients' records.

**Results:** Seven patients with *BRCA1/2*-mutated PDAC were identified. All 7 patients harbor germline mutations (5 *BRCA2*; 2 *BRCA1*), and 2 out of these 7 patients have additional somatic *BRCA2* mutations in their tumor. Mean age at diagnosis was 67.6 (range 54-83 years) and male to female ratio is 5:2. Two out of 7 patients have a personal history of non-*BRCA*-associated malignancy and all 7 patients have a family history of malignancy including *BRCA*-associated malignancies and others. PD-L1 positive expression was identified in 2 out of 4 patients. The genetic alterations detected include 6 frameshift mutations (5 *BRCA2*; 1 *BRCA1*), 2 nonsense mutations (2 *BRCA2*) and one splice site mutation in *BRCA1* (Table 1). Concurrent somatic variants involving *KRAS* (7/7), *TP53* (3/7), *CDKN2A* (2/7), *BAP1* (1/7), *SMARCA4* (1/7), *ARID1A* (1/7), *ROS1* (1/7) and *MYC* amplification (1/7) were also identified. Somatic mutations in these genes have also been reported in the TCGA dataset, and while *KRAS* mutations were present at a higher frequency in our *BRCA*-mutated PDAC cohort versus the non-*BRCA*-mutated TCGA PDAC cohort (100% vs 80.1%,  $p=0.3492$ ) and *TP53* mutations at a lower frequency (42.9% vs 66.7%,  $p=0.2334$ ), these differences were not statistically significant.

Table 1. Molecular features of *BRCA1* (ENST00000471181)/*BRCA2* (ENST00000544455)-mutated PDAC

Patients	Mutations
1	Germline_ <i>BRCA2</i> : p.Gln1429SerfsTer9, <b>Somatic_<i>BRCA2</i>: p.Arg155Ter</b>
2	Germline_ <i>BRCA2</i> : p.Ser3147CysfsTer2
3	Germline_ <i>BRCA2</i> : p.Ser1982ArgfsTer22
4	Germline_ <i>BRCA2</i> : p.Val2969CysfsTer7
5	Germline_ <i>BRCA1</i> : p.Lys653SerfsTer47
6	Germline_ <i>BRCA1</i> : c.5216-1G>A, <b>Somatic_<i>BRCA2</i>: p.His473ThrfsTer6</b>
7	Germline_ <i>BRCA2</i> : p.Phe1870Ter

**Conclusions:** Our set of *BRCA1/2*-mutated PDAC had some unique clinicopathological and molecular features. Mean age at diagnosis for patients with germline *BRCA1/2* variants is similar to the non-*BRCA*-mutated PDAC group reported in TCGA data (mean 64.9), suggesting the incidence of PDAC is lower than other *BRCA*-associated malignancies (e.g. breast and ovarian cancers). While we did not find statistically significant differences in the distribution of concurrent somatic variants in our PDAC compared to TCGA PDAC, possibly due to the small size of our cohort, additional studies may be helpful to further explore biologic differences between *BRCA* mutated and non-mutated PDAC. Interestingly, in addition to *BRCA1/2* germline mutations, some cases carried somatic mutations that are related to DNA damage response pathway (1 *BAP1* and 2 *BRCA2* mutations).

**878 Interobserver Concordance of Tumor Response and Tumor Bed Size in Post-Neoadjuvant Therapy (NAT) Resections for Pancreatic Ductal Adenocarcinoma (PDAC)**

Yoko Matsuda<sup>1</sup>, Keiichi Okano<sup>1</sup>, Takayuki Sanomura<sup>1</sup>, Yuko Nakano-Narusawa<sup>1</sup>, Juanjuan Ye<sup>2</sup>, Masanao Yokohira<sup>1</sup>, Mutsuo Furihata<sup>3</sup>, Chiharu Tanaka<sup>3</sup>, Riko Kitazawa<sup>4</sup>, Yoshimi Bando<sup>5</sup>, Yamato Suemitsu<sup>6</sup>, Motohiro Kojima<sup>7</sup>, Mari Mino-Kenudson<sup>8</sup>, Yasuyuki Suzuki<sup>1</sup>  
<sup>1</sup>Kagawa University, Faculty of Medicine, Kita-gun, Japan, <sup>2</sup>Kagawa University, Faculty of Medicine, Japan, <sup>3</sup>Kochi University, Nankoku, Japan, <sup>4</sup>Ehime University Hospital, Toon, Japan, <sup>5</sup>Shinkura, Japan, <sup>6</sup>Japanese Red Cross Medical Center, Shibuya Ward, Japan, <sup>7</sup>National Cancer Center Hospital, Kashiwa, Japan, <sup>8</sup>Massachusetts General Hospital, Harvard Medical School, Boston, MA

**Disclosures:** Yoko Matsuda: None; Takayuki Sanomura: None; Yuko Nakano-Narusawa: None; Mutsuo Furihata: None; Chiharu Tanaka: None; Yoshimi Bando: None; Yamato Suemitsu: None; Mari Mino-Kenudson: *Consultant*, H3 Biomedicine; *Consultant*, AstraZeneca; *Grant or Research Support*, Novartis; Yasuyuki Suzuki: None

**Background:** Pathology assessments of tumor response after NAT are critical for guiding the selection of adjuvant therapy and improving prognostic stratification in PDAC. However, several tumor response scoring (TRS) systems exist and there have been conflicting reports on their reproducibility as well as prognostic performances. Of the TRS systems, the College of American Pathologists (CAP) grading system is commonly used, and the good

prognostic performance of MD Anderson (MDA) score has been reported. We recently proposed a grading system based on the area of residual tumor (ART) that has shown to be prognostic (Sci Rep, in press). In the present study, we assessed and compared the interobserver concordance of CAP, MDA and ART scoring systems as well as residual tumor and tumor bed sizes. We also analyzed the correlation between pathological assessments and clinical parameters.

**Design: Methods:** This study included 30 patients with PDAC who had undergone post-NAT pancreatectomy (gemcitabine and S-1-based chemotherapies with radiation). Seven pathologists and one senior trainee individually microscopically measured the size of tumor and that of tumor bed, and evaluated TRS in accordance with the CAP, MDA, and ART grading systems. Interobserver concordance among the systems, and the correlation between tumor sizes (on microscopy and by CT scan) and serum tumor markers (CEA and CA-19-9) were determined.

**Results:** 27% of cases showed more than 2 different scores based on ART. Discrepant cases exhibited smaller sizes of tumor and tumor bed than those of concordant cases. The interobserver concordance for ART was higher than MDA and CAP scoring systems (Kendall's coefficient, 0.61, 0.60, 0.50). The interobserver concordance for the microscopic size of residual tumor and that of tumor bed were high (Ebel's interclass correlation coefficient, 0.79, 0.85). A microscopic tumor size/tumor bed ratio correlated with changes in serum markers and post NAT tumor size determined by CT. ART and MDA scores correlated with post NAT tumor size determined by CT.

**Conclusions:** The ART grading system that was designed to be simple and more objective has achieved the highest concordance; thus, it may be most practical for assessing tumor response in post-NAT resections for PDAC. A ratio of tumor size/tumor bed size correlated with the changes in serum markers and post NAT tumor size by imaging studies; thus, it may be a valuable factor that needs to be further evaluated with regard to a prognostic performance.

### **879 Clinicopathologic Characteristics of Metastatic Neoplasms Involving the Extrahepatic Biliary System: Some Usual and Unusual Suspects**

Pooja Navale<sup>1</sup>, Kanchan Kantekure<sup>2</sup>, Monika Vyas<sup>2</sup>

<sup>1</sup>Barnes-Jewish Hospital/Washington University, St. Louis, MO, <sup>2</sup>Beth Israel Deaconess Medical Center, Harvard Medical School, Boston, MA

**Disclosures:** Pooja Navale: None; Kanchan Kantekure: None; Monika Vyas: None

**Background:** Diagnosis of metastatic neoplasms on small biliary sampling can be very challenging, particularly since metastatic neoplasms are rarely considered in the differential diagnosis. The literature on frequency and types of metastatic neoplasms involving the extrahepatic bile ducts (EHBD) is limited. The aim of this study was to describe the clinicopathologic features of metastatic neoplasms involving the EHBD.

**Design:** The pathology archives of 2 institutions were searched for metastatic neoplasms detected in EHBD samples (biopsy and resections). Patient demographic, clinical and radiological information were recorded. Contiguous involvement of the EHBD by regional primaries was excluded. All H&E and immunohistochemical stained slides were reviewed. The histologic features of the neoplasms (morphology and differentiation) were recorded.

**Results:** We found 14 cases, including 7 males, with an average age of 60 years (range: 23-76 years). All but one case, had a prior/concurrent history of malignancy. 3 patients were asymptomatic while rest presented with jaundice, pain, elevated alkaline phosphatase, cholangitis, altered mental status and vomiting. On imaging, 7 cases showed a stricture with dilatation of the bile ducts, 7 showed enhancement/mass. The location of involvement was proximal in 7, distal in 4, and middle in 1 case. Table 1 shows the histologic features of metastatic neoplasms along with their primary sites. 9/12 (75%) cases had concurrent metastases to other sites (most commonly liver, 58%). In 1 case biliary metastasis presented before the lung primary and was misdiagnosed as a biliary primary. The average interval between the primary and biliary metastasis was 44 months (range: 0 to 108). In 1 case, there was a concern for a new biliary primary (interval-108 months). On follow up (average 53 months), 5 patients died of disease with 2 each were alive with and without disease.



Morphologic characteristics	Diagnosis	Primary site
Glandular	Adenocarcinoma	Colon (n=5)
		Gall bladder (n=1)
		Lung (n=1)
Squamoid	Squamous cell carcinoma	Anus (n=1)
		Cervix (n=1)
Poorly differentiated	Melanoma	Skin (n=2)
	Small cell carcinoma	Lung (n=1)
	High grade neuroendocrine neoplasm	Pancreas (n=1)
Clear cell	Clear cell renal cell carcinoma	Kidney (n=1)

**Conclusions:** While diagnosis of metastatic neoplasms in EHBD is rare, metastases from colorectal primary site are most common. In majority of these cases, suspicion for metastatic disease is high due to prior/concurrent metastasis at other sites. Rarely, EHBD metastasis can be the first presentation of malignancy or can present after a long interval, raising concern for a second primary. High index of suspicion and awareness of clinical history is paramount in avoiding a misdiagnosis of primary biliary neoplasm in these cases.

### 880 Long Term Survival in Advanced Pancreatic Adenocarcinoma and New Target Identified by Whole Transcriptome Analysis

Christine Orr<sup>1</sup>, Wael Al Zoughbi<sup>2</sup>, Jones Nauseef<sup>1</sup>, Kevin Hadi<sup>1</sup>, Shaham Beg<sup>1</sup>, Rohan Bareja<sup>3</sup>, David Wilkes<sup>2</sup>, John Stahl<sup>4</sup>, Zenta Walther<sup>4</sup>, Kimberly Johung<sup>4</sup>, Brian Robinson<sup>2</sup>, Jose Jessurun<sup>5</sup>, Andrea Sboner<sup>2</sup>, Allyson Ocean<sup>2</sup>, Olivier Elemento<sup>2</sup>, Marcin Imielinski<sup>6</sup>, Juan Miguel Mosquera<sup>2</sup>, Rohit Chandwani<sup>1</sup>  
<sup>1</sup>New York-Presbyterian/Weill Cornell Medicine, New York, NY, <sup>2</sup>Weill Cornell Medicine, New York, NY, <sup>3</sup>Englander Institute for Precision Medicine, New York, NY, <sup>4</sup>Yale School of Medicine, New Haven, CT, <sup>5</sup>New York-Presbyterian/Weill Cornell Medical Center, New York, NY, <sup>6</sup>Weill Cornell Medicine, New York City, NY

**Disclosures:** Christine Orr: None; Wael Al Zoughbi: None; Jones Nauseef: None; Kevin Hadi: None; Shaham Beg: None; Rohan Bareja: None; David Wilkes: None; John Stahl: None; Zenta Walther: None; Kimberly Johung: None; Brian Robinson: None; Jose Jessurun: None; Andrea Sboner: None; Allyson Ocean: *Consultant*, Tyme Therapeutics; *Speaker*, Daiichi Sanyko; *Consultant*, Celgene; *Advisory Board Member*, Array; Olivier Elemento: *Stock Ownership*, Volastra Therapeutics; *Stock Ownership*, OneThree Biotech; Marcin Imielinski: None; Juan Miguel Mosquera: None; Rohit Chandwani: None

**Background:** Diagnosis of pancreatic ductal adenocarcinoma (PDAC) represents a dismal prognosis (mean overall survival of ~1 year). Patients with pancreatic acinar cell carcinoma (PACC) have a comparatively better prognosis than those with PDAC, yet still worse than pancreatic neuroendocrine tumors. Recurrent *NRG1* fusions in *KRAS* wild-type PDAC have been described. Here we present highlights of whole-genome (WGS), whole-exome (WES), and whole-transcriptome (RNAseq) sequencing analysis of a pancreatic cancer cohort with emphasis on patients with metastatic disease.

**Design:** We studied 55 samples from 48 PDAC patients (38 metastatic, 10 primary) and 3 samples from 1 PACC patient. Median age at diagnosis was 67 years (range 33-78). Male to female ratio was 0.75:1. 75% of patients had distant metastasis at time of diagnosis. Whole-exome sequencing (WES) with algorithms to determine tumor mutational burden (TMB) and microsatellite instability (MSI) status, and RNAseq were performed as part of our IRB-approved NGS-based study. A subset of 12 genomes were also interrogated by state-of-the-art whole-genome-based algorithms (*Cell* 2020). Probability of homologous recombination deficiency (HRD) was assessed via HRDetect. Clinico-pathologic and molecular findings were correlated.

**Results:** All samples tested by MSIsensor were microsatellite stable irrespective of primary or metastatic source. TMB density ranged from 0.027 to 42.13 mutations/megabase (cut-off for high TMB ≥10). High TMB was detected in two metastases (same patient) and one primary. Both PDAC patients with high TMB had long-term survival (3 years and 11 years, respectively). The PACC patient harbored a germline *BRCA1* pathogenic mutation and responded to low-dose FABL0x with long survival (~4 years to date). HRD probability results (by HRDetect) were consistent with data from 12 WGS analyzed: HRD was detected in 2 out of 12 samples in patients with pathogenic *BRCA1* and *BRCA2* mutations. RNAseq identified 35 non-recurrent fusions in 13/25 (52%) tumors analyzed including a novel potentially targetable *KDM4C-JAK2* fusion. We interrogated RNA-seq from pan-cancer

TCGA data (10,967 cases) and confirmed the rarity of this fusion, finding evidence of *KDM4C-JAK2* only in one breast cancer case.

**Conclusions:** We report 1) a rare non-recurrent targetable *KDM4C-JAK2* fusion in PDAC; 2) association of high TMB with significant longer survival (up to 11 years in one case), consistent with reported favorable prognosis for solid tumors; and 3) long-term survival in PACC in a patient with a *BRCA1* germline mutation and favorable response to a novel combination therapy. Further analysis of WGS data is ongoing.

**881 Clinical Validation of Next-Generation DNA Sequencing for Early Neoplastic Risk Assessment of Cystic Pancreatic Lesions: Ultra-Sensitive SafeSeq Molecular Barcoding Technique**

Vamsi Parimi (Parini)<sup>1</sup>, Emily Adams<sup>1</sup>, Aparna Pallavajjala<sup>2</sup>, Jialing Huang<sup>3</sup>, Rena Xian<sup>4</sup>, Christopher Gocke<sup>2</sup>, Ming-Tseh Lin<sup>5</sup>, Bert Vogelstein<sup>6</sup>, James Eshleman<sup>1</sup>

<sup>1</sup>*Johns Hopkins University School of Medicine, Baltimore, MD*, <sup>2</sup>*Johns Hopkins University, Baltimore, MD*, <sup>3</sup>*Thomas Jefferson University, Philadelphia, PA*, <sup>4</sup>*Johns Hopkins Medical Institutions, Baltimore, MD*, <sup>5</sup>*Johns Hopkins Hospital, Baltimore, MD*, <sup>6</sup>*The Ludwig Center for Cancer Genetics and Therapeutics and Sidney Kimmel Comprehensive Cancer Center, Baltimore, MD*

**Disclosures:** Vamsi Parimi (Parini): None; Emily Adams: None; Aparna Pallavajjala: None; Jialing Huang: None; Rena Xian: None; Christopher Gocke: None; Ming-Tseh Lin: None; Bert Vogelstein: *Stock Ownership*, Thrive Earlier Detection, founder of and holds equity.; *Stock Ownership*, Personal Genome Diagnostics, founder of, holds equity in and consultant; *Consultant*, Sysmex; *Consultant*, Consultant and holds equity to Catalio Capital Management and NeoPhore; *Consultant*, Consultant, Eisai, and CAGE Pharma and holds equity in CAGE Pharma; James Eshleman: None

**Background:** Comprehensive molecular characterization of pancreatic cysts resulted in the classification of PC and identified unique somatic alterations among intraductal papillary mucinous neoplasms (IPMN) and mucinous cystic neoplasms (MCN); neoplastic precursors of invasive pancreatic adenocarcinoma (PDAC). Our current lower limit of detection for somatic variant allele frequency (VAF) on clinically validated NGS is 5%. Accurate identification of low-level variants by NGS in PC fluid can result in curative surgical resection and preventing PDAC, the 3<sup>rd</sup> leading cause of death.

**Design:** DNA extraction was performed by tissue homogenizer and sonication methods using the Qiagen AllPrep kit. Qubit and TapeStation are used to quantify the DNA and ddPCR is performed as a reference assay. PDAC cell lines (PANC 502, 504) with well-characterized KRAS G12D & G12V variants are used as controls at varying DNA input concentration, and serial dilutions (variant: normal concentration of 1:100 and 1:1000). Additionally, pancreatic cyst fluid samples are used as part of the clinical validation. Ultra-deep hybrid capture-based NGS assay (NovaSeq IDT probes, xGen Prism library and Kapa Roche Hyper prep kit) using ultrasensitive Safe-Seq unique molecular barcoding (dual UMI-9bp tag) technology and custom UMI family call algorithm is used to improve the sensitivity and to mitigate the PCR amplification errors (NGS noise). Efficiency is defined as total unique reads/estimated input haploid genome molecules x 100. Somatic variants in oncogenes (KRAS, GNAS, BRAF, NRAS, PIK3CA, CTNNB1), tumor suppressor genes (RNF43, CDKN2A, SMAD4, TP53, VHL), LOH status, and cross-contamination indicators (8 genes, 75 SNP loci) are evaluated.

**Results:** Bioinformatics pipeline variant call algorithm using UMI-family calls showed 100% concordance with manual verification using IGV. KRAS G12D & G12V variant detection is successfully made at VAF of 1%, and 0.1%. The variant read depth has increased by 100 fold relative to the current clinical specimen (mean @ 100ng input= 110K reads) and efficiency has increased by 30 fold by molecular barcoding technique. The analytical sensitivity of the NGS based variant detection is 1 in 1,000 (VAF-0.1%).

**Conclusions:** We report the successful utilization of UMI based molecular barcoding technique for the validation process of ultra-sensitive capture-based, NGS approach for the detection of 11 genes in pancreatic cyst fluid samples in a CLIA-accredited laboratory.

**882 Pancreatic Neuroendocrine Neoplasms Frequently Express S100 by Immunohistochemistry**

Michael Pepper<sup>1</sup>, Allison Zemek<sup>2</sup>, Teri Longacre<sup>3</sup>, Brock Martin<sup>4</sup>

<sup>1</sup>Stanford University, Palo Alto, CA, <sup>2</sup>Southern California Permanente Medical Group, Downey, CA, <sup>3</sup>Stanford University, Stanford, CA, <sup>4</sup>Stanford Medicine/Stanford University, Stanford, CA

**Disclosures:** Michael Pepper: None; Allison Zemek: None; Brock Martin: None

**Background:** Neuroendocrine neoplasms are a heterogeneous group of tumors with variable and unpredictable behavior. While most neuroendocrine neoplasms arise from the bronchopulmonary and gastroenteropancreatic systems, for which site-specific classification and grade criteria exist, they may be encountered at essentially any site. Prior studies evaluated the role of immunohistochemistry in diagnosing, classifying, and predicting behavior for neuroendocrine neoplasms; however, S100 protein expression has not been assessed in this regard. This study evaluated S100 expression in a large cohort of primary and metastatic neuroendocrine neoplasms of various origins.

**Design:** S100 expression was analyzed in 982 neuroendocrine neoplasms (523 primary, 459 metastatic) on a tissue microarray of 604 patients. Of neoplasms with a known primary site of origin, 39.5% were from pancreas, 26.6% from small bowel, 14.4% from lung, 9.6% from colorectum, 8.0% from stomach, and 1.9% from appendix. Of Ki-67 graded gastroenteropancreatic neuroendocrine tumors, 280 (69.7%) were grade 1, 98 (24.4%) grade 2, and 24 (6.0%) grade 3. Immunohistochemistry for S100 (rabbit polyclonal, Agilent Technologies) was performed on a Leica BOND-III platform at 1:1000 dilution following antigen retrieval using Leica enzyme pretreatment. S100 expression was assessed by a gastrointestinal pathologist and scored semi-quantitatively (0-3+) according to the intensity and extent of nuclear and cytoplasmic staining. Expression was defined as at least weak nuclear staining in ≥5% of neoplastic cells.

**Results:** S100 was expressed in 207/983 (21.1%) of all neoplasms to varying degrees: 1+, 77/207 (37.2%); 2+, 55/207 (26.6%); 3+, 75/207 (36.2%). Of neoplasms with known site of origin (n=749), S100 expression was present in 140/296 (47.3%) from pancreas (p <0.001 vs non-pancreatic), 15/199 (7.5%) from small bowel, 16/108 (14.8%) from lung, 12/60 (20.0%) from stomach, 13/72 (18.1%) from colorectum, and 0/14 (0%) from appendix. Of neoplasms with moderate to strong expression in >50% of neoplastic cells (3+), 66/72 (91.7%) were of pancreatic origin (specificity= 98.7%).

**Conclusions:** In neuroendocrine neoplasms, strong, diffuse, nuclear and cytoplasmic staining for S100 is a specific but insensitive marker of pancreatic origin. Unexpected S100 reactivity may represent a potential diagnostic pitfall in the immunohistologic evaluation of small biopsy specimens. Correlation with outcome data is needed to determine clinical/prognostic significance of S100 expression.

**883 Somatostatin-Derived Amyloidosis: A Novel Type of Amyloidosis Associated with Well-Differentiated Neuroendocrine Tumors**

Samar Said<sup>1</sup>, Benjamin VanTreeck<sup>1</sup>, Surendra Dasari<sup>1</sup>, Paul Kurtin<sup>1</sup>, Jason Theis<sup>1</sup>, Samih Nasr<sup>1</sup>, Lizhi Zhang<sup>1</sup>, Saba Yasir<sup>1</sup>, Rondell Graham<sup>1</sup>, Ellen McPhail<sup>1</sup>

<sup>1</sup>Mayo Clinic, Rochester, MN

**Disclosures:** Samar Said: None; Benjamin Van Treeck: None; Surendra Dasari: None; Paul Kurtin: None; Samih Nasr: None; Lizhi Zhang: None; Saba Yasir: None; Rondell Graham: None; Ellen McPhail: None

**Background:** Amyloidosis is a group of diseases that results from extracellular deposition of misfolded proteins with a beta-pleated sheet structure. There are currently 36 proteins known to form amyloid in humans. The associated clinical features are determined in part by the identity of the amyloidogenic protein. Using mass spectrometry-based proteomics (LC/ MS MS), we identified an index case of somatostatin-type amyloidosis associated with a well differentiated neuroendocrine tumor involving duodenal ampulla.

**Design:** Following identification of the index case, we queried our reference laboratory database of 19,298 amyloid specimens from myriad anatomic sites typed by mass spectrometry-based proteomics (LC/ MS MS) and identified



3 additional cases of somatostatin-related amyloidosis. For all cases, histologic examination with hematoxylin and eosin and Congo red stained slides was performed and available clinical data were reviewed.

**Results:** The results are shown in Table 1. The cohort consisted of 4 adults (2 females, 2 males). Age at diagnosis ranged between 47 and 73 years. All cases showed amyloid deposition (confirmed with Congo red stain), associated with well-differentiated neuroendocrine tumor and some showed features of somatostatinoma such as pseudoglandular and trabecular architecture and psammoma bodies. The tumor/amyloid was located in the duodenal ampulla (2 cases), distal duodenum/proximal jejunum (1 case) and pancreas (1 case). A mass lesion was noted in 3 cases while enlarged ampulla was the indication for biopsy in the remaining case. Laser microdissection of congophilic amyloid material followed by analysis by LC MS/MS demonstrated abundant spectra for proteins associated with amyloids of all types (apolipoprotein A IV, apolipoprotein E, and serum amyloid P component) confirming the diagnosis of amyloidosis in all cases. In addition, there were abundant spectra corresponding to somatostatin indicating that the amyloid is somatostatin-related. There was no spectral evidence for other amyloid precursor proteins.

Case #	Age	sex	Specimen type	location	Associated tumor	Other related findings
1	63	M	FNA with cell block	Pancreas	Well differentiated neuroendocrine tumor	Pancreas mass/cyst
2	60	M	Biopsy	Duodenum, ampulla	Well differentiated neuroendocrine tumor	1.9 cm mass, NF1, multiple neurofibromas
3	47	F	Biopsy	Duodenum, ampulla	Well differentiated neuroendocrine tumor	Enlarged ampulla
4	73	F	Resection	Distal duodenum/ Proximal jejunum	Well differentiated neuroendocrine tumor	4 cm mass

**Conclusions:** Somatostatin-derived amyloidosis is a previously-unrecognized type of amyloidosis, associated with well-differentiated neuroendocrine tumors of the pancreas and duodenum.

**884 Incidental Biliary Dysplasia in the Gallbladder: How Many More Blocks Should We Submit?**

Christopher Sande<sup>1</sup>, Kevin Trowell<sup>1</sup>, Jacob Sweeney<sup>1</sup>, Zhaohai Yang<sup>2</sup>

<sup>1</sup>Hospital of the University of Pennsylvania, Philadelphia, PA, <sup>2</sup>University of Pennsylvania Perelman School of Medicine, Philadelphia, PA

**Disclosures:** Christopher Sande: None; Kevin Trowell: None; Jacob Sweeney: None; Zhaohai Yang: None

**Background:** Incidental biliary dysplasia or carcinoma can be seen in cholecystectomy specimens. When initially submitted sections show dysplasia, additional sampling is often performed to rule out carcinoma. However, no consensus exists regarding the number of additional blocks required or whether the entire gallbladder needs to be submitted, and literature on this topic is sparse. We retrospectively reviewed cases of incidental dysplasia and carcinoma of the gallbladder and correlated with clinical outcomes to ascertain the number of blocks necessary to rule out carcinoma.

**Design:** A query of our institution’s database identified cases diagnosed as gallbladder dysplasia or carcinoma over a 13-year period. Cases with a prior diagnosis of biliary carcinoma or a grossly identified mass lesion in the gallbladder were excluded. All slides were reviewed to confirm the diagnosis on initially and subsequently submitted blocks, the number of subsequently submitted blocks, and any change in diagnosis based on subsequently submitted blocks. The medical record of each patient was reviewed for any subsequent diagnosis of biliary cancer.

**Results:** Of 7711 cholecystectomy patients, 33 met the inclusion criteria, including 12 males and 21 females with a mean age of 58 years. Seven cases were diagnosed as invasive carcinoma, all on initially submitted blocks and within the first 2 blocks. Of 20 cases with low grade dysplasia (LGD) on the initial blocks, 5 (25%) were upgraded to high grade dysplasia (HGD) on subsequently submitted blocks, all diagnosed within the first 4 blocks. Six cases had an initial diagnosis of HGD, all of which were made within the first 3 blocks. Of the patients with LGD or HGD on initial blocks, the gallbladder was entirely submitted for 22/26, requiring an average of 14 blocks (range 9-35), and none were found to have carcinoma, including 2 cases with diffuse HGD. Clinical follow-up was available for

17/26 patients with a final diagnosis of LGD or HGD, none of whom developed biliary cancer with a mean follow-up of 44 months (median 21, range 4-108).

**Conclusions:** In this study, incidental carcinoma of the gallbladder was diagnosed within the first 2 submitted blocks. With an initial finding of LGD, 25% were upgraded to HGD on subsequently submitted blocks, and all HGD was diagnosed within the first 4 blocks. No patient with a final diagnosis of LGD or HGD developed carcinoma. Thus, when initially submitted blocks show biliary dysplasia, a total of 4 blocks may be sufficient to make a clinically relevant diagnosis, and entire submission of the gallbladder is not warranted.

### **885 Deep Proteomic Characterization of Non-Ductal Pancreatic Neoplasms Reveals Distinct Subtypes and Molecular Pathways**

Atsushi Tanaka<sup>1</sup>, Makiko Ogawa<sup>1</sup>, Kei Namba<sup>1</sup>, Ronald Hendrickson<sup>1</sup>, David Klimstra<sup>1</sup>, Michael Roehrl<sup>1</sup>  
<sup>1</sup>Memorial Sloan Kettering Cancer Center, New York, NY

**Disclosures:** Atsushi Tanaka: None; Makiko Ogawa: None; Kei Namba: None; Ronald Hendrickson: None; David Klimstra: None; Michael Roehrl: None

**Background:** There are few studies that apply deep pan-proteomic approaches to pancreatic tumors, especially to non-ductal entities. Moreover, previous transcriptome studies will have likely missed targetable proteins because global correlation between mRNA abundance and quantitative protein expression is generally low. This motivated us to perform mass spectrometric pan-proteomic analyses of rare pancreatic tumor types and to identify protein signatures and proteome-based subtypes.

**Design:** We selected 77 non-ductal pancreatic tumors, including 39 well differentiated pancreatic neuroendocrine tumors (PanNETs), 11 acinar cell carcinomas (ACCs), 12 pancreatoblastomas (PBLs), and 15 solid pseudopapillary neoplasms. Total proteomes were extracted from formalin-fixed paraffin embedded tissue and analyzed by liquid chromatography tandem mass spectrometry using a high-resolution Orbitrap Fourier transform instrument. Protein identification and label-free quantification were performed with MaxQuant. We performed unsupervised classification, differential expression analyses, and protein pathway enrichment analyses. To uncover therapeutic vulnerabilities of each entity, we searched drug-protein interactions by using the drug-gene interaction database (DGIdb).

**Results:** We detected 8,309 proteins in these samples. Of these proteins, 4,798 proteins were shared by all entities. We found entity-specific proteins for each disease, ranging from 245 to 625. Unsupervised clustering of all lesions clearly separated each entity and also discovered novel proteomic subtypes within each entity. To elucidate proteomic differences between PBLs and ACCs, whose histologies can mimic each other, we performed differential analyses and found 149 up-regulated proteins and 172 down-regulated proteins in PBLs vs. ACCs, shedding light onto oncogenic pathway differences at protein level. We also performed UMAP analyses of PanNETs and found distinct proteomic subtypes, including new clusters of G1/G2 PanNETs that might be used for proteome-based outcome prediction of these tumors.

**Conclusions:** Global deep proteomics by mass spectrometry can identify proteomic subtypes that are invisible to DNA/RNA-based methods. Our approach may provide better pathologic classification, understanding of oncogenesis, and potential prognostic biomarkers that are specific to non-ductal pancreatic tumors. Proteomics may enable us to tailor the treatment of these tumors and can provide solutions for analogous problems in many other cancers.

### **886 The Extension Beyond the Pancreas with Closer Correlation to N Status Should be Re-Included to Define T Category in Pancreatic Carcinoma**

Jana Tarabay<sup>1</sup>, Ahmad Charifa<sup>2</sup>, Sherehan Zada<sup>2</sup>, Vishal Chandan<sup>3</sup>, Xiaodong Li<sup>4</sup>

<sup>1</sup>University of California, Irvine, Irvine, CA, <sup>2</sup>UCI Medical Center, Orange, CA, <sup>3</sup>University of California, Irvine, Orange, CA, <sup>4</sup>UCI Medical Center, South Pasadena, CA

**Disclosures:** Jana Tarabay: None; Ahmad Charifa: None; Vishal Chandan: None; Xiaodong Li: None

**Background:** In the new 8<sup>th</sup> edition of AJCC cancer staging system, the peripancreatic involvement has been replaced by tumor size to define T stage. Nodal status has also been divided into N1 and N2 based on number of positive lymph nodes. However, the concept of "extension beyond the pancreas" has been suggested to be re-investigated in a recent study. The aim of this study is to compare and evaluate the feasibility of the new T and N stages for 8<sup>th</sup> AJCC Staging System of pancreatic cancers.

**Design:** 101 cases of pancreatic adenocarcinomas from Whipple resection were retrieved (January 1, 2010 to June 30, 2017). The correlation of clinical outcomes with T stage and N status from both AJCC 7<sup>th</sup> and 8<sup>th</sup> classifications were analyzed.

**Results:** The median age was 64 years (range 32 to 91 years) with male/female ratio of 1.65:1. 26 (25.7%) cases were grade 1, 41(40.6%) grade 2, 32(31.7%) grade 3, and 1(1%) grade 4. Tumor size ranged from 1 mm to 10.5 cm (mean =3.08). 78 (77.2%) cases showed positive LVI, 91(90.0%) cases were positive for PNI and 25 cases had at least one positive margin. The followup time was up to 10 years.

Using AJCC 7<sup>th</sup> edition, 8 (7.9%) patients were classified as pT1, 5 (4.9 %) pT2, and 88 (87.1%) as pT3. 74 cases had positive lymph nodes. 4 of 13 pT1 or pT2 tumors had positive lymph nodes while 70 of 88 T3 tumors had positive lymph nodes (Table 1, Fisher test,  $p=0.0007$ ). Using 8<sup>th</sup> edition, no pT1 or T2 tumors were upgraded; however, 59 (67%) of the pT3 tumors were downgraded into pT1a (1), pT1b (1), PT1c (7) and pT2 (50). 74 pN1 tumors were also sub-staged into N1 (48) and N2 (26). 46 of pT1 or pT2 tumor had 72 positive lymph nodes while 27 of 29 pT3 tumor had positive lymph nodes (Table 1, Fisher test,  $p= 0.0028$ ). More tumors with positive lymph nodes have been staged as pT1 in 7<sup>th</sup> than 8<sup>th</sup> edition (3/8 vs. 10/17); 3 of seven new staged pT1 tumors had more than 3 positive lymph nodes (N2). In addition, substaging nodal status in 8<sup>th</sup> edition provided more stratified prediction of clinical outcome between N1 and N2 groups with Kaplan-Meier analysis (Log-Rank,  $p=0.0359$ ).

Table1. The correlation of T and N stage of pancreatic adenocarcinoma by both 7<sup>th</sup> and 8<sup>th</sup> editions of AJCC

	7 <sup>th</sup> AJCC			8 <sup>th</sup> AJCC		
	pT1 or pT2	pT3		pT1 or Tp2	pT3	
<b>Positive Lymph nodes (n)</b>	4	70	$p=0.0007$	46	27	$p= 0.0028$
<b>Negative Lymph nodes (n)</b>	9	18		26	2	

**Conclusions:** High percentage of previously staged pT3 tumors (59 of 88) has been down staged toT2, or even to pT1 tumor and 72% had positive lymph nodes. Moreover, the T stage by 7<sup>th</sup> edition guide shows closer correlation to N status ( $P$  value: 0.0007 vs 0.0028). The result of our study suggests that tumor extension beyond the pancreas should be re-included to define T stage.

**887 Histopathologic Infiltration Pattern Predicts Metastasis and Progression Better than pT-Stage and Grade in Well-Differentiated Pancreatic Neuroendocrine Tumors: A Proposal for an Infiltration-Based Morphologic Grading System**

Orhun Taskin<sup>1</sup>, Michelle Reid<sup>2</sup>, Pelin Bagci Culci<sup>3</sup>, Serdar Balci<sup>4</sup>, Ayse Armutlu<sup>5</sup>, Deniz Demirtas<sup>5</sup>, Burcin Pehlivanoglu<sup>6</sup>, Burcu Saka<sup>7</sup>, Bahar Memis<sup>8</sup>, Emine Bozkurtlar<sup>3</sup>, Can Berk Leblebici<sup>9</sup>, Adelina Birceanu Corobea<sup>10</sup>, Yue Xue<sup>11</sup>, Mert Erkan<sup>5</sup>, Yersu Kapran<sup>5</sup>, Cenk Sokmensuer<sup>12</sup>, Aldo Scarpa<sup>13</sup>, Claudio Luchini<sup>13</sup>, Olca Basturk<sup>14</sup>, N. Volkan Adsay<sup>15</sup>

<sup>1</sup>Koç University, Istan, Turkey, <sup>2</sup>Emory University Hospital, Atlanta, GA, <sup>3</sup>Marmara University, Istanbul, Turkey, <sup>4</sup>Independent Consultant, Turkey, <sup>5</sup>Koç University, Istanbul, Turkey, <sup>6</sup>Basaksehir Cam and Sakura City Hospital, Istanbul, Turkey, <sup>7</sup>Istanbul Medipol University, Istanbul, Turkey, <sup>8</sup>SBU Sisli Hamidiye Etfal Training and Research Hospital, Istanbul, Turkey, <sup>9</sup>Hacettepe University, Turkey, <sup>10</sup>Clinical Hospital Sfanta Maria Bucuresti, Bucharest, Romania, <sup>11</sup>Northwestern University Feinberg School of Medicine, Chicago, IL, <sup>12</sup>Hacettepe Üniversitesi Tip Fakültesi, Ankara, Turkey, <sup>13</sup>University of Verona, Verona, Italy, <sup>14</sup>Memorial Sloan Kettering Cancer Center, New York, NY, <sup>15</sup>Koç University Hospital, Istanbul, Turkey

**Disclosures:** Orhun Taskin: None; Michelle Reid: None; Pelin Bagci Culci: None; Serdar Balci: None; Ayse Armutlu: None; Deniz Demirtas: None; Burcin Pehlivanoglu: None; Burcu Saka: None; Bahar Memis: None; Can Berk Leblebici: None; Adelina Birceanu Corobea: None; Yue Xue: None; Mert Erkan: None; Aldo Scarpa: None; Claudio Luchini: None; Olca Basturk: None; N. Volkan Adsay: None



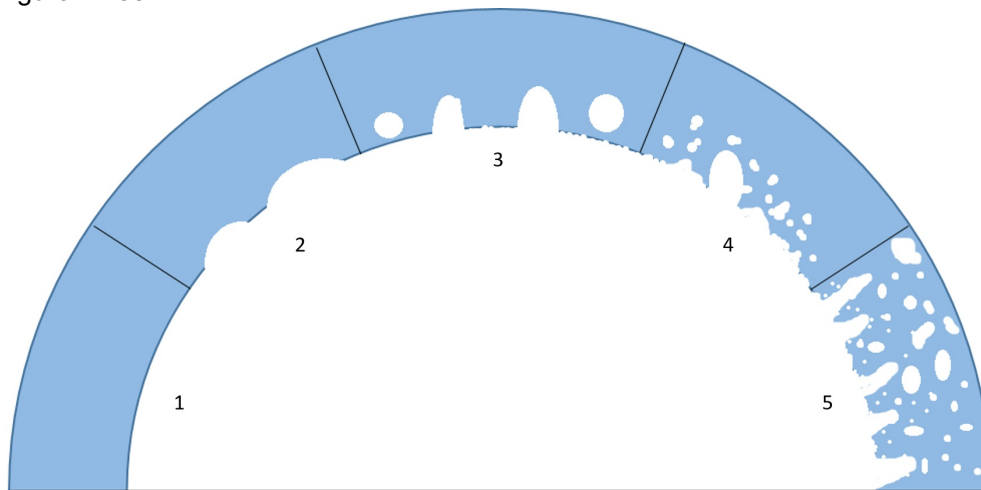
**Background:** Advancing edge profile is a powerful representation of tumor behavior in many organs, the most striking example being the endocrine organs such as thyroid where it is the ultimate determinant of the final diagnosis (adenoma vs minimally invasive vs widely invasive carcinoma) and management.

**Design:** In this study, a grading system was developed and tested in 181 pancreatic neuroendocrine tumors (PanNETs). Three tumor slides representative of the spectrum (least, medium and most) of invasiveness at advancing edge were selected in each case, and each slide was scored as: Well-demarcated/encapsulated as 1 point; Mildly irregular and/or minimal infiltration into adjacent tissue, 2 points; Infiltrative, several clusters beyond the main tumor but still relatively close and/or satellite demarcated nodules, 3 points; No demarcation, several cellular clusters away from the tumor, 4 points; Highly infiltrative, scirrhous, dissecting the normal parenchymal elements, 5 points. Cases with scores of 3 to 5 were defined as “non/minimally infiltrative” (NI; n=77), 6-9 as “moderately infiltrative” (MI; n=68), and 10-15 as “highly infiltrative” (HI; n=36). The findings were correlated with adverse outcome (metastasis, progression or death).

**Results:** This grading system showed strong statistically significant correlation with every established sign of aggressiveness (Ki67 index, grade, tumor size and pT-stage; see Table 1). More importantly, in multivariate analysis incorporating Ki67 index and pT-stage, this proposed system was found to be the most significant predictor of adverse outcomes with HI group showing odds ratio (OR) of 16.4 compared to NI (95% CI 5.182-52.286; p<0.001), and MI over NI of 3.9 (95% CI 1.577-10.002; p=0.003). pT-stage was less strong, with pT3/4 OR over pT1 as 8.2 (95% CI 2.908-23.582; p<0.001), and pT2 over pT1 being 3.1 (95% confidence interval 1.054-9.371; p=0.04). As importantly, for tumors <2 cm, for which watchful waiting is employed nowadays, the rate of progression increased significantly with invasiveness: 1/28 (4%) in NI, 7/27 (26%) in MI and 4/8 (50%) from HI, both emphasizing the applicability of this scoring system for this important group as well as its size independence.

	<b>Non/minimally infiltrative (Score &lt;6)</b>	<b>Moderately infiltrative (Score 6-9)</b>	<b>Highly infiltrative (Score &gt;9)</b>	<b>p-value</b>
<b>n (%)</b>	77 (43%)	68 (37%)	36 (20%)	
<b>Mean age, year (SD)</b>	53.8 (14.5)	56.1 (15.1)	52.3 (17.1)	0.534
<b>F/M</b>	1.3	1.1	1.2	0.854
<b>Grade (%)</b>				
<b>G1</b>	71%	52%	23%	<0.001
<b>G2</b>	26%	43%	62%	
<b>G3</b>	3%	5%	15%	
<b>Mean Ki-67 index (SD)</b>	3.6 (4.6)	6.6 (13.5)	9.5 (9.9)	<0.001
<b>Mean size, cm (SD)</b>	3 (2)	3.4 (2.3)	4 (2.4)	0.095
<b>pT stage (%)</b>				
<b>pT1</b>	39%	38%	14%	0.031
<b>pT2</b>	33%	21%	31%	
<b>pT3</b>	28%	41%	52%	
<b>pT4</b>	0%	0%	3%	
<b>Presence of PNI (%)</b>	15%	23%	69%	<0.001
<b>Presence of LVI (%)</b>	31%	47%	71%	<0.001
<b>Lymph node metastasis (%)</b>	12%	36%	62%	<0.001
<b>Liver/distant metastasis (%)</b>	12%	22%	39%	0.015

Figure 1 - 887



**Conclusions:** In PanNETS, tumor invasiveness at the advancing edge has strong, independent prognostic value, which is even stronger than grade and stage, is easily applicable in routine practice, and therefore should be considered for incorporation into pathology reports and management algorithms. It can be of particular value in stratifying the ever-problematic “watchful waiting” group (< 2 cm).

**888 GRP78 Expression and Prognostic Significance in Treated and Treatment-Naïve Patients with Pancreatic Ductal Carcinoma**

Yi Tat Tong<sup>1</sup>, Hua Wang<sup>1</sup>, Dongguang Wei<sup>1</sup>, Laura Prakash<sup>1</sup>, Michael Kim<sup>1</sup>, Ching-Wei Tzeng<sup>1</sup>, Jeffrey Lee<sup>1</sup>, Asif Rashid<sup>1</sup>, Robert A. Wolff<sup>1</sup>, Anirban Maitra<sup>1</sup>, MH Katz<sup>1</sup>, Huamin Wang<sup>1</sup>

<sup>1</sup>The University of Texas MD Anderson Cancer Center, Houston, TX

**Disclosures:** Yi Tat Tong: None; Dongguang Wei: None; Ching-Wei Tzeng: None; Asif Rashid: None

**Background:** Glucose-regulated protein 78 (GRP78) plays an essential role in protein folding, transportation, and degradation, thus regulating ER homeostasis and promoting cell survival, proliferation and invasion. A recent study showed a positive correlation between GRP78 expression and poor prognosis in treatment-naïve patients with pancreatic ductal adenocarcinoma (PDAC). However, GRP78 expression in PDAC patients who received neoadjuvant therapy has not been reported. The aims of this study is to compare GRP78 expression between the treated and treatment-naïve PDACs and to correlate it with survival in both cohorts.

**Design:** Our study included two cohorts of PDAC patients: 125 treated patients and 140 treatment-naïve patients. Immunohistochemical staining for GRP78 was performed on tissue microarrays (TMAs) using a rabbit anti-human GRP78 antibody (1:150 titer). Since GRP78 expression was diffuse in all positive cases, the staining results were scored based on the intensity as 0 (no staining), 1 (weak), 2 (moderate), 3 (strong). Statistical analyses were performed.

**Results:** GRP78 expression scores of 0, 1, 2, and 3 were detected in 15, 71, 35, and 19 treatment-naïve PDAC patients and 39, 57, 16, and 13 treated PDAC patients, respectively. The expression of GRP78 was higher in treatment-naïve patients compared to those in treated patients ( $p < 0.001$ ). In treated cohort, disease-free survival (DFS) and overall survival (OS) were 11.5 months and 30.1 months, respectively, for patients with GRP78 positive PDACs, compared to 19.2 months ( $p = 0.08$ ) and 40.8 months ( $p = 0.03$ ), respectively, for those with GRP78 negative PDACs. In addition, GRP78 expression correlated with higher frequency of recurrent/metastasis ( $p = 0.045$ ). In treatment-naïve cohort, patients with GRP78 positive tumors had shorter DFS ( $p = 0.008$ ) and OS ( $p = 0.02$ ) than those with GRP78 negative tumors. In multivariate analysis, tumor response grading ( $p = 0.04$ ), ypN ( $p = 0.005$ ) and GRP78 expression ( $p = 0.03$ ) were independent prognostic factors for OS in treated cohorts. GRP78 expression was also an independent prognostic factor for both DFS ( $p = 0.03$ ) and OS ( $p = 0.049$ ) in treatment-naïve cohort.

**Conclusions:** Our study showed that GRP78 expression in treated PDAC patients is lower than that in treatment-naïve patients. GRP78 expression correlated with shorter OS in both treated and treatment-naïve PDAC patients and shorter DFS in treatment-naïve PDAC patients. Our findings suggest that targeting GRP78 may help to improve the prognosis in PDAC patients.

### **889 Mucinous Carcinoma of Gallbladder: A Series of 32 Cases from a Single Tertiary-Care Oncology Center**

Subhash Yadav<sup>1</sup>, Surbhi Lahoti<sup>1</sup>, Mukta Ramadwar<sup>1</sup>, Kedar Deodhar<sup>1</sup>, Rajiv Kumar<sup>1</sup>, Munita Bal<sup>2</sup>

<sup>1</sup>Tata Memorial Hospital, Mumbai, India, <sup>2</sup>Tata Memorial Centre, Mumbai, India

**Disclosures:** Subhash Yadav: None; Surbhi Lahoti: None; Mukta Ramadwar: None; Kedar Deodhar: None; Rajiv Kumar: None; Munita Bal: None

**Background:** Mucinous carcinoma of the gallbladder (MCGB) is a rare histologic subtype of gallbladder carcinoma (GBC), defined by the presence of > 50% stromal mucin. Since its first report in 1986, < 50 cases of MCGB have been reported, with the majority being isolated case reports. Little is known about the clinicopathologic spectrum of MCGB.

**Design:** Clinical data and pathologic material of all cases of MCGB diagnosed from 2008-2019 were retrieved and the histologic diagnosis was confirmed in accordance with the WHO 2019 i.e., cases with the presence of >50% stromal mucin were defined as MCGB. Clinical and treatment details were recorded from the electronic medical records.

**Results:** Thirty-two cases of MCGB were identified from a total cohort of 4400 cases of GBC registered at our institute forming 0.8% of our total cohort of GBC cases. The average age of patients was 57.3 years and there was a striking female-to-male ratio of 7:1. Fifty percent of patients presented with acute cholecystitis. Gallstones were noted in 16 patients. The average tumor size was 3.4 cm (range, 1.5-7cm). Histologically, there were 11 conventional mucinous carcinoma (>50% stromal mucin), 3 colloid carcinoma (>90% stromal mucin), 13 signet ring cell adenocarcinoma (>50% signet ring cells), and 5 cases of mixed mucinous-signet ring cell carcinoma (<50% signet ring cells). The majority of tumors were poorly-differentiated (n=22) while others were moderately-differentiated. Calcification was identified in 8 cases. There were 15.6% R1 cases. There were 26%, 30% and 44% patients in pT2a, pT2b, and pT3 stage, respectively. Lymph node metastasis was seen in 31%. Biliary intraepithelial neoplasia was seen in 5 cases (4 low-grade and 1 high-grade). Adjuvant chemotherapy, chemoradiation, and neoadjuvant chemoradiation were received in 50%, 19%, and 3%, respectively. The mean follow-up duration was 13.4 months (median 9 months, range 5-31 months). 37.5% of patients developed distant metastasis, while 13 patients died of disease, with the majority of the deaths occurring in the first two years. The median overall survival was 9 months (mean 11.1 months, range 5-26 months).

**Conclusions:** MCGB is an extremely rare and highly aggressive variant of GBC characterized by striking female proclivity, presentation as acute cholecystitis, advanced pathologic stage, and poor outcomes.

### **890 SMARC-Deficient Pancreatic Undifferentiated Carcinomas**

Aslihan Yavas<sup>1</sup>, Jaclyn Hechtman<sup>1</sup>, N. Volkan Adsay<sup>2</sup>, Michelle Reid<sup>3</sup>, Jinru Shia<sup>1</sup>, David Klimstra<sup>1</sup>, Olca Basturk<sup>1</sup>

<sup>1</sup>Memorial Sloan Kettering Cancer Center, New York, NY, <sup>2</sup>Koç University Hospital, Istanbul, Turkey, <sup>3</sup>Emory University Hospital, Atlanta, GA

**Disclosures:** Aslihan Yavas: None; Jaclyn Hechtman: None; N. Volkan Adsay: None; Michelle Reid: None; Jinru Shia: None; David Klimstra: None; Olca Basturk: None

**Background:** Inactivating alterations in subunits of Switch/Sucrose non-fermentable chromatin remodeling complex (SWI/SNF) genes have been described as possibly the driver event in various tumor types. Recent studies focusing on SMARC subunits of this complex have also shown that SMARC-mutant tumors may be more sensitive to immunotherapy. For the pancreas, there is very limited data on this topic.

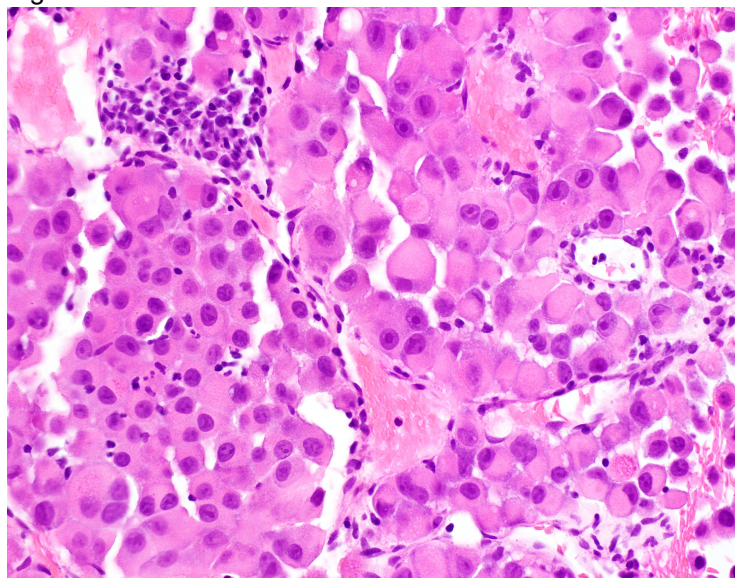


**Design:** We identified 14 SMARC-deficient pancreatic undifferentiated carcinomas and analyzed their clinicopathologic, immunohistochemical (IHC, with the SMARC-related proteins of INI-1, BRM and BRG1, and MMR proteins) and genomic characteristics using 410-468 gene next-generation sequencing (NGS). By mean of comparison, 29 SMARC-retained pancreatic undifferentiated carcinomas as well as 96 consecutive conventional pancreatic ductal adenocarcinomas (PDACs) were also analyzed.

**Results:** Patients with SMARC-deficient pancreatic undifferentiated carcinomas were predominantly male (71%) with a mean age of 54 years (range, 38-72). Mean tumor size was 5.2 cm (range, 1.7-10). Follow-up information was available for 13 patients; 1 died of post surgical complications, 7 DOD at median 5 months and 5 were alive at median 8 months (4 with disease). Microscopically, all 14 tumors revealed predominantly rhabdoid morphology (vs in 9/29 of SMARC-retained pancreatic undifferentiated carcinomas) and expressed cytokeratin at least focally. Glandular (ordinary adenocarcinoma) component was identified only in 3/14 (vs in 21/29 of SMARC-retained pancreatic undifferentiated carcinomas). By IHC, INI1 (SMARCB1) protein expression was lost in 8 cases, BRM (SMARCA2) in 3, and BRG1 (SMARCA4) in 2. One case had both INI1 and BRM expression loss. MLH1 and PMS2 protein expression loss was detected in only 1 undifferentiated carcinoma with BRM expression loss. In contrast, none of 96 PDACs showed SMARC-related or MMR expression loss. NGS analysis was performed in 6 SMARC-deficient pancreatic undifferentiated carcinomas and 89 PDACs: 3/4 SMARC-deficient pancreatic undifferentiated carcinomas with INI1 expression loss by IHC were found to have *SMARCB1* deletions and the 4th case revealed *SMARCB1* copy number changes. Since the NGS panel employed did not include *SMARCA2*, status of this particular gene could not be determined in 2 SMARC-deficient pancreatic undifferentiated carcinomas with BRM expression loss. However, 1 of these cases had a *SMARCA4* missense mutation without related BRG1 expression loss. Only 1/89 PDACs revealed a *SMARCA4* missense mutation.

	SMARC-deficient pancreatic undifferentiated carcinomas (n:14)	SMARC-retained pancreatic undifferentiated carcinomas (n:29)	Pancreatic ductal adenocarcinomas (n:96)
Mean age, years (range)	54 (38-72)	65 (42-82)	69 (33-88)
Male/Female, %	71/29	45/55	55/45
Head/Body-Tail, %	54/46	52/48	75/25
Mean tumor size, cm (range)	5.2 (1.7-10)	5.4 (1.6-14)	3.8 (1.3-9.4)
Median follow-up, months (range)	5 (1-62)	17 (4-175)	15 (1-44)

Figure 1 - 890



**Conclusions:** Although not specific, rhabdoid morphology appears to be associated with SMARC-deficiency in pancreatic undifferentiated carcinomas. Recognition and appropriate subtyping of this rare and aggressive variant might become necessary for future therapeutic strategies.